Journal of Polymer Science

WILEY

JOURNAL OF POLYMER SCIENCE

REVIEW OPEN ACCESS

Basalt Fiber Reinforced Polymers: A Recent Approach to Electromagnetic Interference (EMI) Shielding

Umar Naseef Mohamed Fareez[1] | Aymen Loudiy[1] | Mustafa Erkartal[2] | Cagatay Yilmaz[1]

[1]Department of Mechanical Engineering, Faculty of Engineering, Abdullah Gül University, Kocasinan/Kayseri, Turkey | [2]Department of Basic Sciences, Faculty of Engineering, Architecture and Design, Bartin University, Bartin, Turkey

Correspondence: Cagatay Yilmaz (yilmaz.cagatay@agu.edu.tr)

Received: 9 August 2024 | **Revised:** 18 September 2024 | **Accepted:** 19 September 2024

Funding: The authors received no specific funding for this work.

Keywords: basalt fibers | EMI | FRP | post treatment

ABSTRACT

Electromagnetic wave (EMW) radiation pollution is getting more severe as result of the advancement of electronic technology. Researching shielding materials with superior EMI (electromagnetic interference) shielding characteristics is therefore crucial. Basalt fibers (BFs) have been an emerging candidate in the fiber-reinforced polymer (FRP) category due to their favorable mechanical and chemical properties, along with being favorites in sustainability and having low production costs. Therefore, due to the rising need for cheaper and efficient alternatives in the EMI shielding industry, the EMI shielding is covered in terms of BF composite materials and their properties in this review, starting with the EMI shielding mechanism and followed by how BF composites affect the EMI properties. This review then covers the post-treatments of BF composites and, finally, the factors of the composites that affect the EMI properties. Moreover, the EMI shielding applications in which BFRPs are used are comprehensively discussed as well. This review aspires to bridge an understanding between EMI shielding as a material property and the BF composites that are developed to aid in the EMI shielding application.

1 | Introduction

EMI or electromagnetic interference is the effect of electromagnetic waves (EMWs) on external objects, where the waves are not restored to their initial position when they are propagated. EMWs have the same direction and propagation of their magnetic and electric fields thereby making it more accessible to transfer the energy in areas of magnetic and electric fields and can propagate through any medium such as solid, liquid, gas or even a vacuum. As EMWs have an electric field that is alternating due to an alternating magnetic field, they produce EMI [1].

Many applications today require the consideration of EMI when they are being processed. Since the digitalization of technology from the 20th century, many electronic devices have become a household necessity. Thus, it has become crucial to consider EMI that has become an issue on many fronts such as defense, corporate, medical, and environmental sectors. In the defense industry, EMI has become a tool for espionage, as well as damaging conventional weapons [2]. EMI could be exploited by hackers to gain valuable and confidential information as well [3]. The medical industry suffers from the risk that EMI causes the human body, such as the irreversible effect on the central nervous system (CNS) if it is exposed long-term to EMW [4]. The environmental sector can be affected as well due to the EMI effect on precision instruments used for the weather which can cause major consequences when measuring important factors such as temperature, humidity, wind speed, and so forth [5].

EMI shielding is the process of enclosing an electrical circuit, also known as an EMI emitter or susceptor, partially or entirely using a shield (a shaped conducting substance). As a result, it

affects both how much EMI energy created by the circuit can escape into the external environment and how much EMI radiation from the external environment may enter the circuit [6]. Shielding has been accomplished using several materials with various electrical conductivity, magnetic permeability, and geometries. In addition to lowering EMI emissions, shielding also offers a separate ground reference, which significantly lowers internal crosstalk, circuit path coupling, and total common mode coupling. Shielding is also used to reduce electrostatic discharge (ESD) and thus, electric potential, as well as to absorb microwave radiation. In shielding housings and enclosures made of plastic or other nonconductive materials, many commercial electronic equipment is packed [6, 7].

To provide shielding, these enclosures must be coated with a conductive substance if the devices are required to rely on enclosure shielding for electromagnetic compatibility (EMC) compliance. Vacuum deposition, electroless plating, arc spray, and conductive spray paint are some of the metalizing methods used in this application. The latter method, a slurry of metal particles in a carrier that resembles paint, is most usually employed. Conductive substances such as silver, nickel, copper, or carbon are highly present in these conformal coatings as extremely small particles, and shielding efficiency levels between 60 and 100 dB [7–10].

Moreover, metallized fabrics can provide an amalgamation of qualities that are proving to be very valuable in a wide range of EMI shielding solutions, including effective shielding performance, convenience in manufacturing, transparency to air, partial transparency to visible light, and low specific weight, the attributes of a fabric remain unchanged after metallic treatment; they include drape, texture, tear strength, shrinkage, elongation, and other features [7]. For example, to improve their EMI shielding abilities, basalt fibers are frequently combined with other substances like polyvinyl alcohol (PVA) or metal fibers [11–13]. They are also utilized in a variety of other products, such as construction materials, composite materials, and parts for the automotive and aerospace industries.

Leading materials that have been used in EMI shielding have carbon fibers [14–17], copper fibers [18], nickel-coated [19, 20] and silver-coated fibers [21], conductive polymers [22, 23], and metallic foams [24, 25], due to their high electrical conductivity and shielding effectiveness. Moreover, the recent surge of composite materials in the EMI shielding sector to provide optimal shielding properties while maintaining desirable mechanical and physical characteristics have resulted in a boom in the further development of hybrid composites [26, 27], metal-matrix composites [28, 29], graphene, graphite, and metal-coated glass fiber-reinforced composites [30–32]. Another recent group of materials used for EMI shielding are the bio-based materials such as cellulose fibers [33, 34], carbon-focused materials extracted from natural products [35], and natural textiles [36].

Fiber-reinforced polymers (FRPs) have gained traction in recent years due to their integration of different properties suitable for the required application. For EMI shielding, the electromechanical properties are a main factor during the material selection process. Fiber composites have been reinforced with conductive materials in order to have favorable electromechanical properties for use in EMI shielding. Basalt fiber-reinforced polymers (BFRPs), a direct competitor to carbon fiber-reinforced polymers (CFRPs) and glass fiber-reinforced polymers (GFRPs), have gained traction in the EMI shielding industry due to their sustainable manufacturing methods, and provided advantageous benefits in terms of EMI shielding properties [37–39]. Regarding electrical properties, basalt fiber composites exhibit relatively low electrical conductivity due to the insulating nature of basalt fibers, making them suitable for electrical insulation and electromagnetic shielding applications [40, 41]. In terms of magnetic properties, basalt fiber composites generally display non-magnetic behavior, as basalt fibers themselves are non-magnetic and do not significantly alter the magnetic properties of the composites [42].

BFRPs also have been an economically and environmentally viable for EMI shielding applications compared to their competitors CFRPs and GFRPs. They are made from naturally occurring basalt rock thereby leading to lower production costs and less energy-intensive processing methods. This aligns with sustainability goals due to less energy consumption and less emissions. Moreover, basalt fiber can be recycled and display a reduced carbon footprint throughout their lifecycle [43], thus effectively portraying advantages over other types of fibers as well. These benefits make basalt fiber composites a promising choice for EMI shielding applications, combining both economic and sustainability considerations for improved performance.

This paper focuses on the EMI shielding aspect of basalt fibers and their composites. While review papers have been focusing on carbon fibers, metals, and nanofibers, with respect to their application in EMI shielding, we will focus on the advantages of basalt fiber composites and the materials that are associated with them, along with the processes and techniques that are used to infuse these materials on the fibers, and how it affects EMI shielding. We will also discuss the EM properties and the properties of the materials that affect EMI shielding.

1.1 | Basalt Fibers

Basalt fibers (BF), shown in Figure 1a, have been used since the early twentieth century, being patented by Frenchman Paul Dhé [44], for applications that surround the civil industry such as public infrastructure and construction [45]. The major advantage, along with favorable elastic modulus, being light and ductile, is the exclusion of the brittle behavior present in carbon fiber (CF) composites that causes stress concentrations along the material [46]. CF production is also more expensive, which means that less load is used in the process [47]. BF composites eradicate the issue because of the hybridization which uses ductile material layers instead of carbon layers [48].

Basalt is a rich natural compound that comprises around 90% of all volcanic rock on Earth [49]. Basalt is very similar to glass, sharing common properties such as lack of electrical conductivity, thermal resistance, and high strength. However, it has more favorable properties such as poor chemical reactivity allowing it to be more resistant to strong chemical bases as opposed to glass which is resistant to strong chemical acids [50]. Basalt has

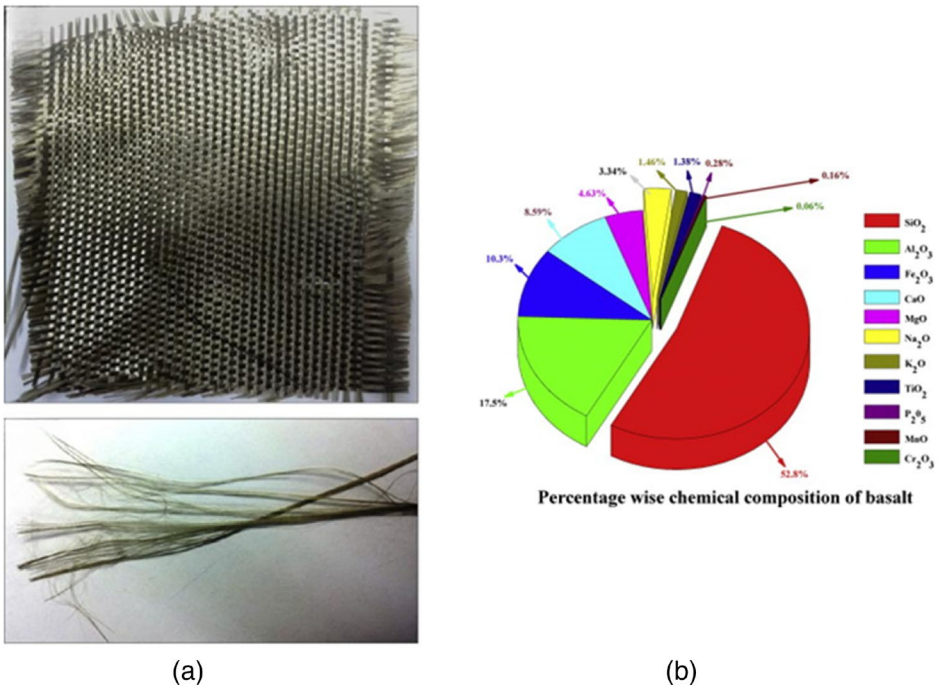

FIGURE 1 | (a) Basalt fiber and strands of BF, (b) Chemical composition of basalt. *Source:* Adapted with permission [46]. Copyright 2015, Elsevier.

a chemical composition consisting of SiO_2, Al_2O_3, MgO, CaO, FeO, Fe_2O_3, N_2O, K_2O, TiO_2, P_2O_5, MnO, and Cr_2O_3 with varying levels of percentages of these compounds [46, 51, 52], as shown in Figure 1b. Alkaline basalts contain around 42% SiO_2, while mildly acidic basalts have around 43%–46% SiO_2, and acidic basalts over 46% SiO_2 [53]. They vary in their physical appearance, ranging from colors such as brown and gray to light green according to the aforementioned chemical composition [54]. The structure of basalt is similar to that of glass; therefore, the physical properties are shared, such as brittleness, chemical and thermal resistance. Basalt fibers are manufactured by methods such as the Junkers method (a melt blowing production technique), which produces short-fiber basalt fibers and the spinneret method which produces continuous-fiber basalt fibers [55, 56].

The Junkers process is a melt blowing manufacturing method. The key element of the method is the transfer of the melt, that goes up to 1580°C, from the gas-heated furnace to a fiberizing device with a horizontal shaft and three centrifugal heads. The lava that had been adhered to the heads falls off due to centrifugal force, and because of the blasting, viscous liquid breaks down into fibers 60–100 mm long and 6–10 μm diameter [57]. The spinneret method of basalt fiber production involves melting basalt rock at around 1450°C and then extruding the molten basalt through a spinneret, a device with numerous small holes. As the molten basalt passes through the holes, it is stretched and solidified into continuous fibers. This process offers precise control over fiber diameter and length, resulting in uniform, high-quality fibers with enhanced performance characteristics [58]. After extrusion, the continuous fibers are wound onto spools for further processing and use. Like the melt blowing method, the spinneret method requires significant energy input for melting and extrusion but is less energy-intensive than steel production. The carbon footprint of the spinneret method is also relatively low due to the use of basalt as a raw material [59]. Basalt fiber composites possess a range of desirable properties for various applications. In terms of mechanical properties, these composites exhibit high tensile strength, surpassing that of traditional glass fiber composites, owing to the high tensile modulus and ability to withstand significant stress levels of basalt fibers [60–62]. They also demonstrate excellent chemical resistance, making them suitable for use in harsh chemical environments due to their resistance to alkalis, acids, and organic solvents [63]. Additionally, basalt fiber composites display noteworthy thermal stability, withstanding high temperatures without experiencing substantial degradation, which can be attributed to their higher melting point compared to organic fibers [64]. Furthermore, basalt fiber composites possess low water absorption, preserving their mechanical integrity and dimensional stability even in moist environments [65, 66]. Their good fatigue resistance allows them to withstand cyclic loading and repetitive stress without significant performance degradation, making them suitable for applications requiring resistance to repeated mechanical loading [67, 68].

1.2 | Cost and Sustainability

In assessing the viability of basalt fiber composite materials for EMI shielding applications, it is imperative to consider not only their performance characteristics but also their economic feasibility and sustainability compared to conventional alternatives such as CFRPs and GFRPs. Economically, basalt fiber composites present a promising alternative due to their relatively lower production costs compared to carbon fiber composites, which are often associated with high manufacturing expenses. For example, the cost of basalt fibers is estimated to

be around $2.26 per pound, whereas carbon fibers can range from $13.6 per pound [47]. Basalt fibers can be produced at a lower cost compared to carbon fibers, attributed to the availability and affordability of raw materials and less energy-intensive processing methods [69]. Additionally, basalt fibers are derived from naturally occurring basalt rock, offering potential cost advantages over glass fibers, which require energy-intensive processes for extraction and refining [70].

Moreover, sustainability considerations play a pivotal role in evaluating the environmental impact of various fiber composites. Basalt fiber production typically involves lower energy consumption and greenhouse gas emissions compared to carbon fiber manufacturing processes, aligning with sustainability objectives. Furthermore, basalt fibers are inherently recyclable, and exhibit reduced environmental footprint throughout their lifecycle, offering potential advantages over carbon and glass fiber counterparts. The energy consumption for the production of basalt fibers is lower than the energy required for carbon fibers and comparable to that of glass fibers. Additionally, the process of creating basalt fibers generates minimal waste and no toxic byproducts. Leftover materials can often be recycled back into the production process, further minimizing environmental impact. BFRPs also have a lower carbon footprint compared to other materials, such as CFRPs, as they do not involve the use of petroleum-based resins and are derived from a renewable source. The use of renewable energy sources, such as solar or wind power, in basalt fiber production can further decrease emissions and improve sustainability [71]. A sustainability comparison encompassing factors such as raw material availability, energy consumption, and recyclability is crucial for assessing the ecological credentials of basalt fiber composites vis-à-vis other FRPs.

BFRPs are considered an environmentally friendly alternative due to being derived from natural volcanic rock, and presenting similar mechanical properties to CFRPs and GFRPs but with a lower environmental impact. Recently, a study examined the Life Cycle Assessment (LCA) of BFRPs and their environmental impact. BFRPs were compared to CFRPs and GFRPs in terms of their reduced Global Warming Potential (GWP)—the total greenhouse gas emissions over the product's life cycle—and Fossil Resource Scarcity (FRS) – the depletion of fossil fuel resources. BFRPs were compared to stainless steel, galvanized steel, and GFRP bars. It was found the GWP of a BFRP bar was 88% lower than that of stainless steel, 49% lower than galvanized steel, and 44% less than that of a GFRP bar [71]. It was also found in earlier studies the percentage reduction in the environmental impact due to using FRP bars in BFRPs was a 62% reduction in CO_2 emissions [72], while GFRPs had a 43% reduction and CFRPs had 39% reduction [73]. This showcases the sustainable and environment-friendly characteristics of basalt fiber when compared to its competitors.

Moreover, it is important to note that the properties of basalt fiber composites can be influenced by factors such as fiber content, orientation, composite fabrication techniques, and the presence of other conductive or magnetic materials in the composite matrix. Tailored composite designs may be necessary to optimize these properties for specific applications.

1.3 | EMI

EMI has been an engineering consideration, especially when processing materials. Therefore, the material selection process, which depends on the application of the material, must account for the property of EMI shielding. EMI, which is caused by the propagation of EMWs, that consist of the EM spectrum: radio waves, microwaves, infrared light, X-rays, and gamma-rays, in order of increasing frequency and decreasing wavelength as shown in Table 1. When an EMW strikes a material, there are three phenomena that occur, called reflectance (R), absorption (A), and transmittance (T) [74, 75]. These three occurrences take place outside or inside the material interchangeably. For example, when an EMW is incident on an object, there is a reflected wave, and the part of the wave that is absorbed, is internally reflected and transmitted, thereby causing multiple reflections sometimes of the same, singular EMW. This occurs multiple times for transmittance as well [76].

Since EMI is based off electromagnetic waves, it is important to study certain properties that would affect EMI shielding. These are shielding effectiveness (SE), electrical conductivity, and the dielectric constant, which is the ability of an insulator to store electrical energy [78]. Moreover, the mechanical properties are tested to check whether they are affected by improving EMI shielding properties.

The shielding efficiency (SE) of the material is used to identify the shielding capacity (attenuation) of the material, usually

TABLE 1 | The classification of EMWs with different frequency and wavelength [77].

Spectral region	Frequency region (Hz)	Wavelength (m)
Radio waves	$1.0 \times 10^{8} - 1.0 \times 10^{5}$	$1.0 - 1.0 \times 10^{3}$
Microwave	$1.0 \times 10^{11} - 1.0 \times 10^{8}$	$0 - 1.0 \times 10^{1}$
Infrared light	$1.2 \times 10^{14} - 1.0 \times 10^{11}$	$2.5 \times 10^{-6} - 1.0 \times 10^{-3}$
Visible light	$7.5 \times 10^{14} - 4.0 \times 10^{14}$	$4.0 \times 10^{-7} - 7.5 \times 10^{-7}$
Ultraviolet light	$1.0 \times 10^{15} - 7.5 \times 10^{14}$	$2.0 \times 10^{-7} - 4.0 \times 10^{-7}$
X-rays	$1.0 \times 10^{20} - 1.0 \times 10^{16}$	$1.0 \times 10^{-12} - 1.0 \times 10^{-10}$
γ-rays	$> 1.0 \times 10^{20}$	$< 1.0 \times 10^{-12}$

found in decibels (dB). It is used in a comparative analysis test to measure the electric field strength before the material shielding is applied and afterward. Therefore, the total shielding efficiency is shown with Equation (1) as the incident electromagnetic wave intensity over the outgoing electromagnetic wave intensity [23, 79, 80]:

$$SE_T = 10\log\left(\frac{P_i}{P_0}\right) \tag{1}$$

$$SE_T = SE_A + SE_R + SE_M \tag{2}$$

Moreover, according to Schelkunoff's theory, the shielding efficiency can be divided into subcomponents that are attenuations of absorption, reflection and multiple internal reflections [81–83] as seen in Equation (2). These components are mathematically shown in the following equations (Equations (3), (4), and (5)).

$$SE_A = -8.68t\frac{\sqrt{f\mu_r\sigma_T}}{2} \tag{3}$$

where t is the thickness of the shielding material, μ_r is the relative permeability of the material, σ_T is the total conductivity and f is the frequency of the electromagnetic waves. In Equation (4), ϵ is the electric permittivity as shown below.

$$SE_R = -10\log\left(\frac{\sigma_T}{16f\epsilon\mu_r}\right) \tag{4}$$

It is known that when EMWs are incident on an object, they undergo multiple internal reflections within the object itself albeit being the lowest EMW attenuation as compared to SE_A and SE_R [84].

$$SE_M = 20\log\left(1 - 10^{\frac{SE_A}{10}}\right) \tag{5}$$

However, it can be found from the equation above Equation (5) that if the SE_A is high (more than 15 dB [80, 85–87]), the value of SE_M can become much smaller to the point that with thick materials, it becomes negligible in the calculation of SE_T, since materials with large thicknesses often have higher absorption values and thus high value of SE_A.

Moreover, the factors that affect SE are permeability, thickness and conductivity as can be deduced from the above equations [88, 89]. The filler materials that are used to adjust for conductivity are examined by these factors, and also portray magnetic and electric dipoles that result from the magnetic and electric phases that the material goes through. Materials that have electric dipoles weaken the impedance of the material and this increases the reflection of the EMWs within. However, the presence of magnetic dipoles causes magnetic loss, which is the sum of the eddy current loss, the magnetic hysteresis loss and the residual loss, which improves the EMI shielding [90].

The distance required for EMW attenuation to 37% or inverse of the exponential of the shield is called skin depth (δ) as shown in Equation (6) [91]:

$$\delta = \frac{1}{\sqrt{\pi f\mu\sigma}} \tag{6}$$

The reflection of EMWs surface and inside the material are dissipated into thermal energy [78, 92]. The absorption of EMWs within the material also do not necessarily play a role in the reduction of transmittance which can take place due to reflection within the material [93]. Therefore, in monolithic isotropic materials, where the properties of a material are constantly independent of the direction, the absorption is found in terms of the reflection and measured transmittance as shown in Equation (7) [94].

$$A = 1 - R - T \tag{7}$$

Moreover, another important parameter to evaluate the absorption potential of a material is the reflection loss. The reflection loss as shown in Equation (8) assesses the amount of power lost when an EM wave reflects off a boundary that typically is between two materials with opposing electrical properties, usually a metal surface and a non-metal one [95]. This is useful to account for investigating the EMI due to the potential mitigation of the amount of energy that penetrates an enclosure or that which propagates to crucial areas. It is given as:

$$RL = 10\log\frac{P_R}{P_I} = 20\log\left|\frac{z_{in} - z_0}{z_{in} + z_0}\right| \tag{8}$$

where P_I and P_R are the incident and reflected powers of the EMWs, respectively. Moreover, z_{in} and z_0 are the impedance of the absorber material and the characteristic impedance of free space, respectively. In the context of electromagnetic wave absorbers, when reflection loss (RL) is represented as a negative value, such as −10 dB, it indicates that only 10% of the incident electromagnetic power is reflected, highlighting that 90% of the energy is absorbed by the material. This means that the higher the negative number, the higher the degree of reflection.

Achieving nearly perfect impedance matching $\left(z_0/z_0 \approx 1\right)$ in an ideal absorber EMI shield is crucial for minimizing reflection and facilitating the efficient penetration of incident electromagnetic waves (EMWs) into the shielding material. This strategy, although challenging to achieve, involves designing structures with similar relative complex permeability $\left(\mu_r = \mu' - \mu''\right)$ and relative complex permittivity $\left(\varepsilon_r = \varepsilon' - \varepsilon''\right)$ values, prioritizing the reduction of reflected EMWs [96].

Assessing the performance of an electromagnetic absorber entails not only evaluating its impedance matching capabilities but also considering its effectiveness in attenuating the EMWs that manage to penetrate the shielding. Real components of complex

permittivity (ε') and permeability (μ') indicate energy storage, while imaginary components $(\varepsilon''\text{and}\,\mu'')$ represent losses such as heat dissipation. The dielectric and magnetic loss capabilities of shields are commonly quantified using $\tan\delta_\varepsilon = \varepsilon''/\varepsilon'$ and $\tan\delta_\mu = \mu''/\mu'$ in combination with the attenuation constant, offering insights into their overall effectiveness in EMI mitigation [97].

In terms of energy dissipation through electric mechanisms, dielectric loss is crucial in evaluating the absorption capability of EMI shields. It involves the dissipation of EMW energy via the movement of electric dipoles and charge carriers, including conduction loss from electron activity (Ohmic loss) and polarization loss from dipole alignment. Influenced by the electromagnetic field's frequency, the material's conductivity, and the mass of polarized species, dielectric loss is measured using the dielectric constant (ε), where the real component (ε') indicates charge storage and the imaginary component (ε'') signifies energy dissipation as shown in Equations (9) and (10) [98, 99].

$$\varepsilon' = \varepsilon_\infty + \frac{\varepsilon_s - \varepsilon_\infty}{1 + (2\pi f)^2\tau^2} \tag{9}$$

$$\varepsilon'' = \frac{2\pi f(\varepsilon_s - \varepsilon_\infty)}{1 + (2\pi f)^2\tau^2} + \frac{\sigma}{2\pi f\varepsilon_0} \tag{10}$$

Here ε_0, ε_s, and ε_∞ refer to the dielectric constants in a vacuum, static state, and at infinite frequency, respectively, while τ is the relaxation time the—time taken for a polarized species to return to its normal state [100].

Furthermore, the losses in the shields also include the reflection loss of the EMI shielding material, multiple reflection and absorption losses as shown in Figure 2. Basalt fibers are insulating by default which does not support EMI shielding therefore they would require a filler material that is conductive. This would require different methods and techniques to form a conductive layer on the fiber surface. In this paper we look at the different methods to form them and the problems that arise with such methods and techniques.

1.4 | EMI Shielding Methods

EMI shielding methods and techniques have varied based on the level of precision needed, the components employed, and the purposes for which they would be needed. For testing purposes for EMI shielding, four approaches are typically used: open field or free space method, shielded box method, shielded room method, and coaxial transmission line method [101–104].

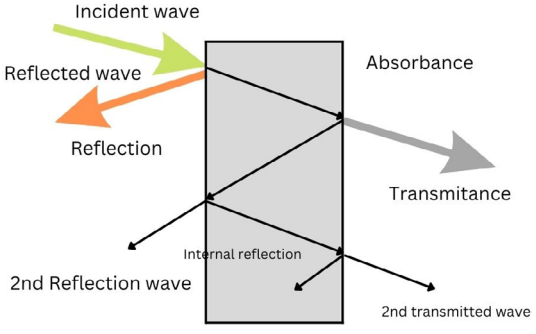

FIGURE 2 | Schematic diagram of the EMI shielding mechanism.

The open field or free space approach, conducted at a distance of thirty meters, is employed for the real-world assessment of electronic assemblies' shielding efficacy, quantifying emitted radiation and transmitted emissions through the power line [104]. In contrast, the shielded box method struggles with achieving proper electrical contact and has a limited frequency range of 500 MHz. Overcoming these challenges, the shielded room method employs larger test specimens, often reaching sizes of 2.5 m^2, in anechoic chambers [101]. However, the coaxial transmission line method offers consistent results across laboratories, with a dynamic range of roughly 80 dB, enabling the decomposition of data into reflected, absorbed, and transmitted components [103]. This method provides a comprehensive and efficient evaluation of shielding effectiveness.

2 | Materials

2.1 | Carbon Nanotubes Basalt Fiber

An example of a nanomaterial with distinctive physical and chemical characteristics is carbon nanotubes (CNTs), which have high electrical and thermal conductivity, high mechanical strength, and high chemical stability. For the creation of various types of nanofiber materials with enhanced properties, the combination of CNTs and electrospinning has received extensive study. The creation of CNT-reinforced electrospinning nanofiber mats is one example of how CNTs and electrospinning can work together [105–107]. In comparison to pure electro spun fiber mats, these materials have been shown to have improved mechanical and electromagnetic properties, making them suitable for a range of applications including sensors, energy storage devices, biomedical materials, and finally electromagnetic interference [108].

Furthermore, Chang et al. [109] report the option of the direct growth of carbon nanotubes using chemical vapor deposition (CVD) on the surface of basalt fibers for electromagnetic interference shielding, the result of study reflects a direct effect of the nanocarbon tubes on the electromagnetic interference shielding of the composite, due to the external reflection and internal absorption of electromagnetic waves which mainly depends on the quantity and quality of the carbon nano tubes which in return depends on the hydrogen flow rate during the preparation of the nanocomposite, to explain the effect of the hydrogen flow rate, the authors showed its effects of removing amorphous carbon from the in situ generated mineral nanoparticles from the catalyst surface to ensure the maintenance of the activity of the catalyst, however increasing the flow rate of H_2 beyond the critical concentration the carbon source gets diluted thus affecting the final product's electromagnetic properties negatively, Figure 3 shows the effects of hydrogen flow rate on the sheet's resistance.

Moreover, in a recent follow-up paper to the aforementioned ones, Chen et al. attempted to optimize the treatment methods and evaluate the effects of CNT-coated basalt-fiber fabric

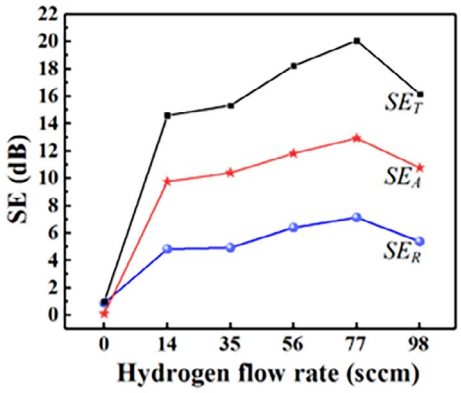

FIGURE 3 | Effect of hydrogen flow rate on SE_T, SE_A, and SE_R values of BFF-CNT77/PDMS sample at 8.2 GHz. *Source:* Reproduced with permission [109]. Copyright 2020, Elsevier.

integrated with PDMS to enhance the EMI shielding efficiency of the nanocomposites. This study, just like the previous one, aimed to utilize the high electrical conductivity of the CNTs and the mechanical advantages of the basalt fibers, to produce enhanced shielding efficiency, across a broad range. CVD was used as the treatment method for uniformly coating the basalt fibers with CNTs to make sure an efficient conductive network was formed within the composite, which was tied down with the PDMS matrix, to ensure flexibility and structural integrity. Experimental measurements revealed that the CNT-coated basalt/PDMS composites achieved an EMI SE of up to 60 dB in the X-band frequency range (8.2–12.4 GHz), surpassing the performance of uncoated basalt/PDMS composites and aligning well with the values reported in the existing literature for similar CNT-based composites. Moreover, this study explored the virtual optimization through COMSOL software to evaluate the electric field intensity, power flow distribution, and electromagnetic wave loss density within the CNT-coated basalt fiber/PDMS nanocomposites, revealing their ability to significantly reduce electric field intensity and power flow, thereby confirming their effectiveness in attenuating electromagnetic energy. The tribological properties were also evaluated such as material thickness, fiber orientation, and CNT coating density which were helpful in optimizing the EMI shielding performance by producing reduction in electric field intensity within the CNT-coated basalt fiber/PDMS nanocomposites by approximately 90% [110].

Mittal et al. [39] used the chemical vapor deposition (CVD) post-treatment process, and just like the previous research investigated the behavior of CNT basalt fiber composites for their electromagnetic shielding properties, but differently from the previous research, the varying parameters were the growth temperature and the synthesis time. To prepare the sample basalt cloth was cleaned with acetone and ethanol, then dried for 2 h at 120°C to prepare the samples. Following that, the fabric was put in a quartz tube reactor to undergo a chemical vapor deposition (CVD) procedure. The fabric was heated to a certain temperature (600°C or 700°C) and maintained at that temperature for a specific amount of time (30 or 60 min) during the CVD process. By adding a mixture of methane and hydrogen gas into the reactor, which then interacted on the surface of the fabric, the CNTs were produced on the basalt fabric, transmission electron microscopy (TEM) and scanning electron microscopy (SEM) were used to examine the surface appearance and structure of the samples. To ascertain the caliber and orientation of the CNTs produced on the basalt fabric, the samples were additionally examined using Raman spectroscopy and X-ray diffraction (XRD). The samples were analyzed after the CNT development procedure to investigate their tribological and electrical properties. The results showed that increasing the temperatures and extending the deposition time during synthesis improved not only the mechanical properties of the composite material but also the electromagnetic shielding interference effectiveness, The ranges of the EMI shielding effectiveness values for BFCNT30/epoxy, BF-CNT60/epoxy, and BF-CNT120/epoxy were 20.70 to 19.71, 23.19 to 24.04, and 30.38 to 28.81 dB, respectively. The team concludes that the increased effectiveness is due to the formation of a complex three-dimensional interconnected conductive network through the insulating epoxy in the samples prepared at higher temperature and for longer time, the results of which the effects of grafting times and temperatures have on shielding effectiveness.

Recent literature examined a composite paper composed of basalt fibers, as shown in Figure 4, aramid nanofibers (ANF), and carbon nanotubes (CNT), that exhibits exceptional properties across multiple domains. With a conductivity of 15.9 S cm^{-1} at 70 wt% CNT content, it demonstrates promising potential for high-performance electromagnetic interference (EMI) shielding. At this composition, the average EMI shielding effectiveness reaches 24.6 dB, blocking 99.65% of incoming electromagnetic waves. Additionally, the paper shows rapid thermal response and high-efficiency electrothermal conversion, with its surface temperature increasing from 71°C to 258°C within 10 s at applied voltages ranging from 6 to 14 V. Its remarkable thermal stability is highlighted by a decomposition temperature of 461°C and 75% mass retention at 800°C in a nitrogen atmosphere. Furthermore, the composite paper maintains its tensile strengths between 16.6 and 17.9 MPa under extreme conditions, such as annealing at 300°C for 6 h, storage for 6 months, immersion in liquid nitrogen for 1 h, and exposure to strong acid and alkali solutions for 24 h [111].

Another recent study presented a novel approach for fabricating sustainable, high-performance, multifunctional fiber-reinforced thermosetting composites (FRTCs) using biobased feedstocks, including basalt fiber (BF), polyvinyl alcohol-grafted-3,4-dihydroxybenzoic acid (P(VA-g-DBA)), and carbon nanotubes/graphene nanoplatelets (CNT&GP). The composite (CBF) exhibited a conductivity of 48.3 ± 7.9 S m^{-1}, with a loading of CNT&GP at 3.3 ± 0.4 wt%. Remarkably, the EMI shielding performance of the CAN/5CBF composite achieved an EMI SE value of 30.4 dB at the X band, corresponding to a shielding efficiency of 99.901%. Additionally, the tensile strength of the CAN/3CBF composite reached 266.0 MPa, while the lap-shear strength of the self-adhered CAN/3CBF composite was 6.5 MPa. Furthermore, the recycled CBF demonstrated a conductivity of 34.8 ± 10.4 S m^{-1}, highlighting the feasibility of closed-loop recycling without significant deterioration in performance [112].

Similarly, the incorporation of Fe_3O_4/CNTs hybrids onto BF surfaces exhibited enhanced EMW absorption capabilities,

attributed to the synergistic effects of interfacial polarization and conduction loss. The BF-Fe_3O_4/CNTs heterostructure, developed through a dip-coating adsorption process, utilizes the synergistic effects of interfacial polarization, conduction loss, magnetic resonance loss, and multiple reflection/scattering to achieve enhanced electromagnetic wave (EMW) absorption. With a 7% addition of CNTs, the composite reaches a minimum reflection loss of −40.57 dB at a thickness of 1.5 mm, demonstrating its superior EMW absorbing properties [113].

All in all, recent advancements in the integration of CNTs with various fiber materials, including basalt and aramid nanofibers, demonstrate the significant potential of these composites for enhanced electromagnetic interference (EMI) shielding and multifunctional applications. Through methods like chemical vapor deposition (CVD) and hybridization with materials such as graphene nanoplatelets and Fe_3O_4, these studies reveal improvements in mechanical properties, conductivity, and EMI shielding effectiveness. For instance, CNT-coated basalt fiber composites are now being considered for use in aerospace components where both EMI shielding and lightweight structural integrity are crucial. Ongoing research continues to optimize fabrication techniques and explore sustainable, high-performance composites, reinforcing the importance of CNT-based materials in next-generation technological applications.

2.1.1 | Graphene

Recently in terms of graphene, a study was conducted where laser-induced graphene (LIG) was generated on polyimide (PI) substrates via laser scribing, creating a porous structure beneficial for composite integration. These LIG-modified PI substrates were then combined with basalt fiber bundles and epoxy resin to form LIG/BF/EP laminates. The porous morphology of LIG facilitated better adhesion and interlocking with basalt fibers, enhancing the composite's mechanical properties. In terms of electromagnetic interference (EMI) shielding, the LIG/BF/EP laminates exhibited significantly improved effectiveness, achieving ~25 dB shielding in 1-layer configurations and ~50 dB in 3-layer configurations across X-band frequencies, highlighting the material's potential for advanced applications in aerospace, automotive, and defense sectors [114].

Current research efforts are focusing on optimizing LIG formation techniques, improving control over its morphology, and enhancing its multifunctional properties, including flexibility, electrical conductivity, and durability. Moreover, recent studies have highlighted LIG's versatility in areas like biosensing, energy storage, and environmental monitoring, where its high conductivity and scalability make it an attractive option [115]. Research is also exploring the combination of LIG with different polymer and fiber matrices to tailor specific properties for advanced engineering applications [116]. This versatility and adaptability keep LIG at the forefront of materials science.

2.2 | Metals

2.2.1 | Copper

Skopintsev et al. [117] studied the effects of metal plated carbon and basalt fiber composites for electromagnetic shielding applications, comparing the effects of carbon, metal plated carbon and metal plated basalt fibers, carbon fibers prepared by pyrolysis of the formed textile structure from manmade or natural fibers, basalt fibers are prepared directly from a melt of a basalt raw material. For the metal plating of carbon fabrics, a standard solution for the electroplating of copper ($CuSO_4 \cdot 5H_2O$ 250, H_2SO_4 75 g L^{-1}) and nickel ($NiSO_4 \cdot 7H_2O$ 300, NaCl 30, H_3BO_3 30 g L^{-1}; pH 5.5), as for basalt copper plating was performed from a solution operating at room temperature and having the following composition: $CuSO_4 \cdot 5H_2O$ 40, potassium sodium tartrate 170, sodium diethyldithiocarbamate 0.01 g L^{-1}; formaldehyde (33%) 20 mL L^{-1}; NaOH to pH 12.5–13. Electroless nickel plating was performed from a solution of the following composition, g L^{-1}: $NiSO_4 \cdot 7H_2O$ (or $NiCl_2 \cdot 6H_2O$) 24, $NaH_2PO_2 \cdot H_2O$ 32, NH_4Cl 27, CH_3COOH 20, and NH_3 (25%) at pH 8.6–8.9. Furthermore, the resistivity of the carbon was found to be reduced from 10 to 0.15 Ω for the copper-plated carbons, thus

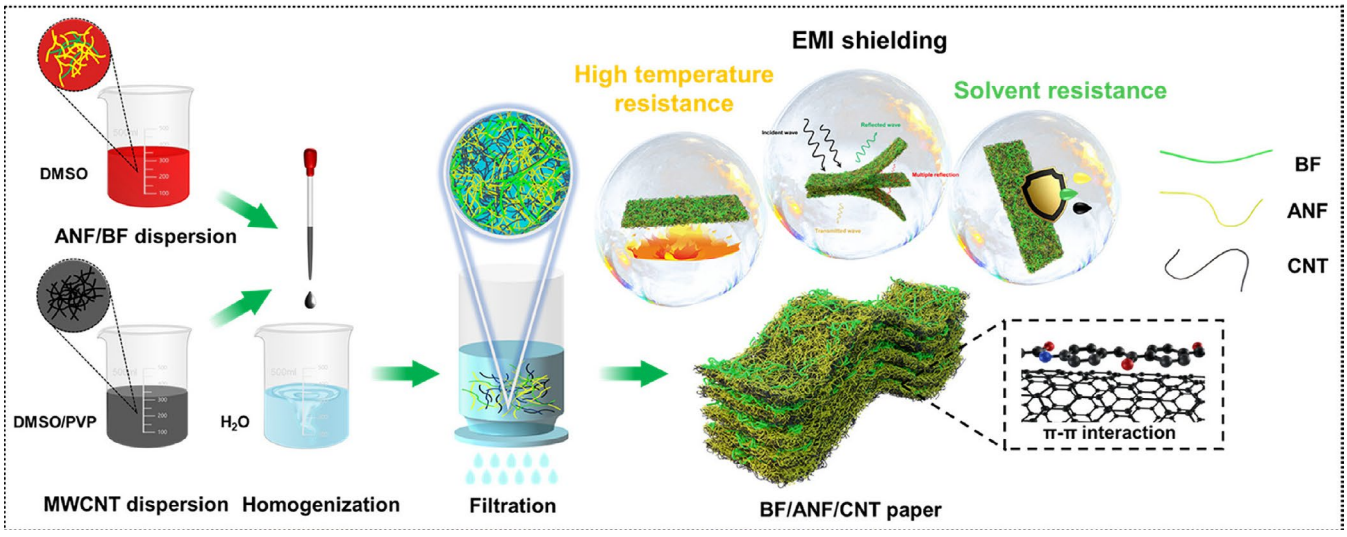

FIGURE 4 | Schematic of the fabrication and treatment method of the BF/ANF/CNT composite paper. *Source:* Adapted with permission [111]. Copyright 2023, ACS Publications.

increasing the shielding effectiveness, noting that the material will be even more expensive. As for the copper basalt fiber composites, it was found that the wt% of copper and coating thickness have the most effect on the effectiveness of the shielding, and longer treatment time translates directly to better shielding performance Figure 5 shows the shielding effectiveness of varying wt% of copper in both near field and plane wave regions of both carbon fibers and basalt fiber. Comparing the two figures in Figure 5, it can be concluded that the metal coated basalt fiber can achieve similar results to metal plated carbon fibers while being less expensive [117].

Yuanjun et al. [10] studied the effect of graphite and silver coated copper powder as a functional filler on continuous basal fibers in terms of electromagnetic shielding properties, wave absorption and dielectric properties. It was found that changing the ratios of graphite and silver coated copper powder has varying effects on the dielectric properties of the composite, as for wave absorption the biggest difference between the different samples with the different composite ratios was found between 1.5 and 1.7 GHz and the sample with the highest performance was the one with the ratio of 2:8 (graphite to silver coated copper fibers), where 90% of the electromagnetic waves were lost, as for shielding properties it was found that the highest performance recorded was in the frequency range of 0.5 to 3 GHz, and the sample has a ratio of 0:10 meaning a purely silver coated copper powder sample, the sample had a shielding efficiency larger than 20 dB.

Utpal et al. [118] studied the electrical properties of multi-walled carbon nanotubes reinforced ethylene methyl acrylate (EMA) nanocomposites and found that the resistivity in the EMA matrix is directly proportional to the content of MWCNTs (multi-wall carbon nanotubes), and that it also increases the conductivity and dielectric constant of EMA, as well as decreasing its electrical resistance similarly to the research of Sayyed et al. [119] on the electrical properties of MWCNT with polystyrene nanocomposites and Nasouri et al. [120] who investigated PVA MWCNTs, Utpal et al. [118] suggest that introducing MWCNT to nanocomposites has promising shielding effects especially in the X-band region.

Recent advancements in copper-plated basalt fiber applications have focused on improving interfacial bonding, developing novel manufacturing methods, exploring multifunctional properties, and addressing environmental sustainability. Researchers have made significant progress in enhancing the adhesion between copper coatings and basalt fibers, leading to improved mechanical properties and shielding performance. Additionally, new manufacturing techniques such as 3D printing and electrospinning have been explored to create complex and customizable structures. Copper-plated basalt fibers are being investigated for applications beyond electromagnetic shielding, including thermal management in electronic devices, structural reinforcement in aerospace, automotive, and construction industries, and energy storage in batteries or supercapacitors. These advancements have opened up new possibilities for the use of copper-plated basalt fibers in various industries, such as electronics, telecommunications, and aerospace. As research continues to progress, we can expect to see even more innovative applications and improved performance of these versatile materials.

2.2.2 | Nickel

Nickel-coated basalt fiber fabric has emerged as a promising material due to its combination of mechanical strength, thermal resistance, and electrical conductivity. The incorporation of nickel coatings enhances the electromagnetic shielding properties of

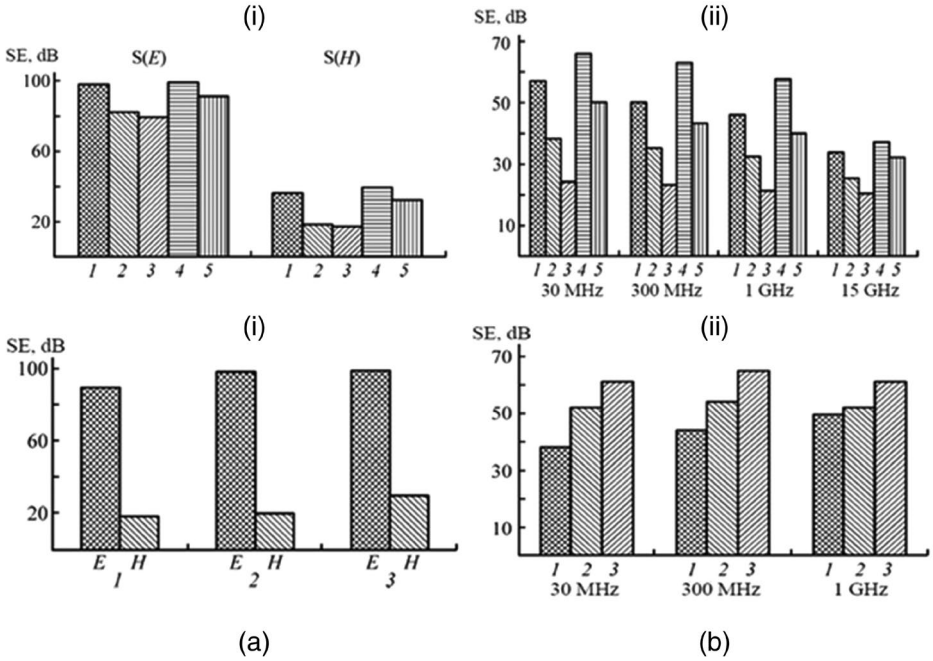

FIGURE 5 | (a) Shielding SE in the (i) near field and (ii) plane wave regions with metal plated basalt fibers. Metal and its content (1) 50% copper (2) 50% nickel (3) 40% nickel (4) 35% copper + 20% nickel (5) 35% copper + 20% nickel cobalt. (b) Shielding SE in the (i) near field and (ii) plane wave regions with carbon fabrics. (1) Carbon fibers, (2) copper plated carbon fabric and (3) nickel plated carbon. *Source:* Adapted with permission [117]. Copyright 2015, Springer.

basalt fiber fabric, making it suitable for applications in electronics, telecommunications, and aerospace.

Skopintsev et al. [117] found that using phosphorus nickel coatings, with approximately 40 wt% relative to the final product, lowered the composite's resistivity to 4.5 Ω. Copper alone showed better shielding efficiency, but a mixture of 35% copper and 20% nickel provided the best results. Kang et al. [121] studied nickel core-shell effects on basalt fiber composites and found that nickel's orientation significantly affects electromagnetic properties, unlike naked basalt fibers. Parallel orientation resulted in high magnetic loss and low dielectric loss, while perpendicular orientation showed the opposite. This difference in dielectric loss is due to nanosized confinement increasing polarization relaxation time, with high magnetic loss mainly from the BF/Ni core-shell heterostructures' magnetic resonance.

Kang et al. [122] also reviewed the effect of varying thicknesses of nickel core basalt fiber composites on its microwave absorption properties; the researchers prepared four samples, those being naked basalt fibers, 70 nm thickness sample, 300 nm thickness sample, 700 nm thickness sample. In terms of microwave absorption naked basalt fibers do not show any effects, In the 9.2–12.4 GHz band for sample A, RL (reflection loss) is greater than 10 dB and rises to over 20 dB. In the whole frequency range that was examined, the RL of sample C is between 5.3 and 7.9 dB. The RL of sample B, however, exceeds 15 dB over the whole X-band and reaches 40 dB at 8.9 GHz. Moreover, Kang et al. [123] explored the effects of pretreatment and processing on nickel core-shell basalt fiber composites synthesized via low-temperature electroless plating. Optimal conditions at 50°C and pH 10.0 increased the fibers' permittivity and electrical conductivity. The core-shell structures exhibited greater dielectric loss tangent and improved X-band microwave absorption capabilities due to enhanced nickel shell conductivity and increased permittivity.

Si et al. [124] synthesized flower-like Ni using a solvothermal method. They dissolved $NiCl_2 \cdot 6H_2O$ and NaOH in ethylene glycol (EG), stirred the mixture, and heated it in a hydrothermal autoclave at 200°C for 10 h. The resulting black precipitates were washed, then dried in a vacuum oven at 60°C. To prepare CB/Ni hybrids, they used an electrostatic self-assembly strategy. They prepared a CTAB solution, added flower-like Ni, and ultrasonically treated it, then combined it with CB solutions in varying ratios (2:1, 4:1, 6:1, 8:1). The mixture was stirred, shaken, centrifuged, and dried at 60°C. For the BF composite, the authors started by cleaning and modifying raw basalt fibers (BF) with polydopamine (PDA). These fibers were then immersed in suspensions containing flower-like Ni, carbon black (CB), or their mixtures, undergoing a dip-coating process repeated five times. The resulting composites, named BF-CB/Ni_2, BF-CB/Ni_4, BF-CB/Ni_6, and BF-CB/Ni_8, varied based on the mass ratios of Ni to CB in the suspensions. The microstructure and absorption properties of the BF composites were controlled by adjusting the mass ratio of Ni/CB in the impregnating solution. BF-CB/Ni_8 exhibited the best electromagnetic wave (EMW) absorption performance, with a minimum reflection loss (RL_{min}) of −35.29 dB and an effective absorption bandwidth (EAB) of 3.25 GHz at a thickness of only 1.5 mm. BF-CB/Ni_6 achieved an EAB of 5.38 GHz with a thickness of 2.5 mm. These enhancements in EMW absorption were attributed to various factors, including efficient reflection/scattering, dipole and interface polarization, magnetic resonance, and eddy current losses.

Korotash et al. [125] investigated basalt fiber composites with graphite and nickel fillers, analyzing their microwave absorption (MWA) properties in the 1.5–2.1 GHz frequency range. They found that MWA depended on filler volume and particle size, with optimal performance observed at approximately 30 wt% filler contents. Anisotropy in MWA was noted due to particle orientation and magnetization directions, with MWA peaking at 30% nickel content for easy magnetization. BF/graphite composites showed higher MWA values compared to BF/nickel composites, although the latter outperformed at low filler concentrations, exceeding BF/graphite by up to 7 times at 10 wt% nickel.

Recent research has focused on optimizing the nickel coating process and exploring new applications for nickel-coated basalt fiber fabric. The development of multifunctional nickel-coated basalt fiber composites is gaining momentum. Efforts are being made to scale up production and reduce costs. Real-world applications of nickel-coated basalt fiber fabric are being explored in electronics, telecommunications, and aerospace industries. Overall, nickel-coated basalt fiber fabric shows great potential for a wide range of applications. As research and development continue, we can expect to see even more innovative and practical uses for this versatile material.

2.3 | Cementous Fibers

Shilang et al. [126] discovered that adding PVA and basalt fibers significantly increased the microwave absorption of cement composites. To study these characteristics, they combined fly ash, cement, and sand in a mixer at a low speed for 1 min while drying. They then added superplasticizer, PVA fibers, basalt fibers, and water, mixing first at a low speed for 60 s, then at a high speed for 2 min. The mixture was poured into oiled steel molds, compacted on a vibrating table for 30 s, cured at 20°C with 95% humidity for 28 days, and dried in an oven at 60°C for 96 h. The authors discovered that the PVA and basalt fibers working together improved the cement composites' microwave absorption capabilities compared to either PVA or basalt fibers working alone. The use of PVA and basalt fibers, according to the authors' findings, can significantly enhance the microwave absorption properties of cement composites containing fly ash and may have potential uses in the fields of microwave absorption materials and electromagnetic wave shielding.

Whereas, another study examined the 3D-printable cementitious composites that contain waste copper solids' electromagnetic and microwave absorbing qualities. Cement, sand, water, and scrap copper solids were the composite materials used in the investigation. A particular weight percentage of waste copper solids was combined with water to create a slurry, which was then used to manufacture the composite. Once the slurry, cement, and sand were combined, the mixture was homogenized. The appropriate shape was then printed out using a 3D printer using the mixture. The samples were subsequently put through a curing process to enable the composite to harden. The printed samples must be cured for 28 days at room temperature in a humid atmosphere. The samples were polished and trimmed to a precise size for

testing after the curing process. By assessing the reflection loss (RL) and electromagnetic interference (EMI) shielding efficiency (SE) over a variety of frequencies, the samples' microwave absorbing qualities were examined. To find out how copper solids affected the composites' ability to absorb microwaves, samples were made with various weight percentages of waste copper solids ranging from 0% to 25%. The electromagnetic and microwave absorbing qualities of the cementitious composites were found to be significantly enhanced by the addition of waste copper solids. Finally, they discovered that the composites' microwave absorption was highly frequency dependent, with the best absorption occurring at a few select frequencies [8].

Ongoing research is focused on exploring new fiber types, optimizing composite formulations, and investigating additional functionalities. The potential applications of cementitious fiber composites extend beyond electromagnetic shielding, including structural reinforcement, thermal insulation, and acoustic absorption. The use of waste materials, such as fly ash and waste copper solids, aligns with sustainability goals and can contribute to a circular economy. Advances in 3D printing and other manufacturing techniques offer opportunities for creating complex and customized cementitious fiber composite structures.

2.4 | Other Materials

In the pursuit of advancing modern communication technologies, research efforts have considered the development of construction materials with multifunctional properties, particularly in the context of electromagnetic wave (EMW) absorption. A spectrum of studies has emerged, each exploring unique methodologies to optimize the electromagnetic properties of various composite materials. Notably, investigations into basalt fiber (BF)-reinforced resin composites have unveiled promising avenues for enhancing EMW absorption performance across the X-band frequency range. By leveraging carbon black (CB) and nano-Fe_3O_4 as absorbents for the absorbing and matching layers respectively, researchers achieved remarkable results, with tailored electromagnetic parameters and layer thicknesses yielding a minimum reflection loss of −43.97 dB and full X-band effective absorption [127]. Additionally, research into white Portland cement (WPC) paste mixed with basalt fiber (BF) analyzed its electromagnetic properties, revealing a decrease in electromagnetic wave reflection rate with increasing BF content, while absorption and transmission rates increased, with the optimum BF volume content for maximum paste strength found to be 0.6%. This study adds to the search for construction materials contributing to 5G signal transmission, crucial for modern communication technologies [128]. These studies collectively underscore the potential of heterostructure composites in advancing EMW absorption materials, offering pathways for improved environmental stability and corrosion resistance.

3 | Post-Treatments

The treatment of basalt fibers to add conductive fillers fits into n array of different methods such as chemical vapor deposition, spray-drying and coating. It is known that the conductive fillers vastly improve the EMI shielding properties compared to that of pure fibers. Therefore, few common methods are considered and how they affect the EMI shielding properties.

3.1 | Chemical Vapor Deposition

Chemical vapor deposition (CVD) is a deposition method by a vapor through chemical reactions between the compound to be deposited and other gases on or towards the substrate to produce a thin film. The matrix is placed in a vacuum inert chamber or tube and heated under a constant rate in the presence of a gaseous mixture (hydrogen, an inert gas and the source gas). Finally, the mixture is removed, and the furnace is brought down to room temperature, with the thin resultant film containing the desired material [129]. Moreover, the layers of deposited material can contribute to improved interfacial polarization and improve the polarization loss of the composites, which would in turn improve EMI shielding capabilities as the dielectric constant would improve due to increased permeability (μ) as there is a charge accumulation at the interface of the heterogeneous structure at lower frequencies—this is called space-charge polarization [130].

Mittal et al. [39] investigated the EM properties of basalt fiber reinforced polymers (BFRPs) with CNTs and epoxy by chemical vapor deposition, which also falls under grafting—a classification of methods that improve the surface area of the fiber to refine the interfacial properties of the fiber. Grafting of the nanofibers allows for a homogeneous distribution of the CNTs along the fiber. Figure 6a explains the preparation of the solution required to catalyze the reaction, followed by grafting through CVD and the final preparation of the BF-CNT/epoxy composites. $C_6H_8O_7$ (Citric acid), $Fe(NO_3)_3$ (Ferric nitrate) and $Ni(NO_3)_2$ (Nickel nitrate) was added to deionized water to form an aqueous solution. NH_4OH is then added to the solution to keep the pH between 8 and 10, and the solution is heated to 60°C to form the nickel ferrite solution. Afterwards, the fiber fabric was dipped in the solution and kept to dry overnight in an oven at 60°C. After the drying process, the sample was taken to the CVD chamber where Ar and H2 gases were introduced at flow rates of 500 and 200 sccm, respectively. The temperature was then increased to the growth temperature which depended on the sample to be produced—at 600°C, 650°C, or 700°C. CH4 was then introduced into the chamber to produce the CNTs at a deposition time which also depended on the sample that was produced—30, 60 or 120 min. After the deposition time, the heat was removed and so were the Ar and CH4 gas supplies. Epoxy resin and hardeners were then added, along with thermal curing and hot pressing at 80°C to finalize the composite. The BF-CNT samples were prepared with respect to growth times and temperatures. Moreover, the results as seen in Figure 6b show that longer deposition times correlate with higher electromagnetic interference shielding efficiency (EMI SE) due to improved dielectric constant and increased permeability (μ) from charge accumulation at heterogeneous structure interfaces, indicating significant potential for advanced EMI shielding applications.

Mittal et al. [131] reported on their follow-up study using chemical vapor deposition (CVD) to compare previously

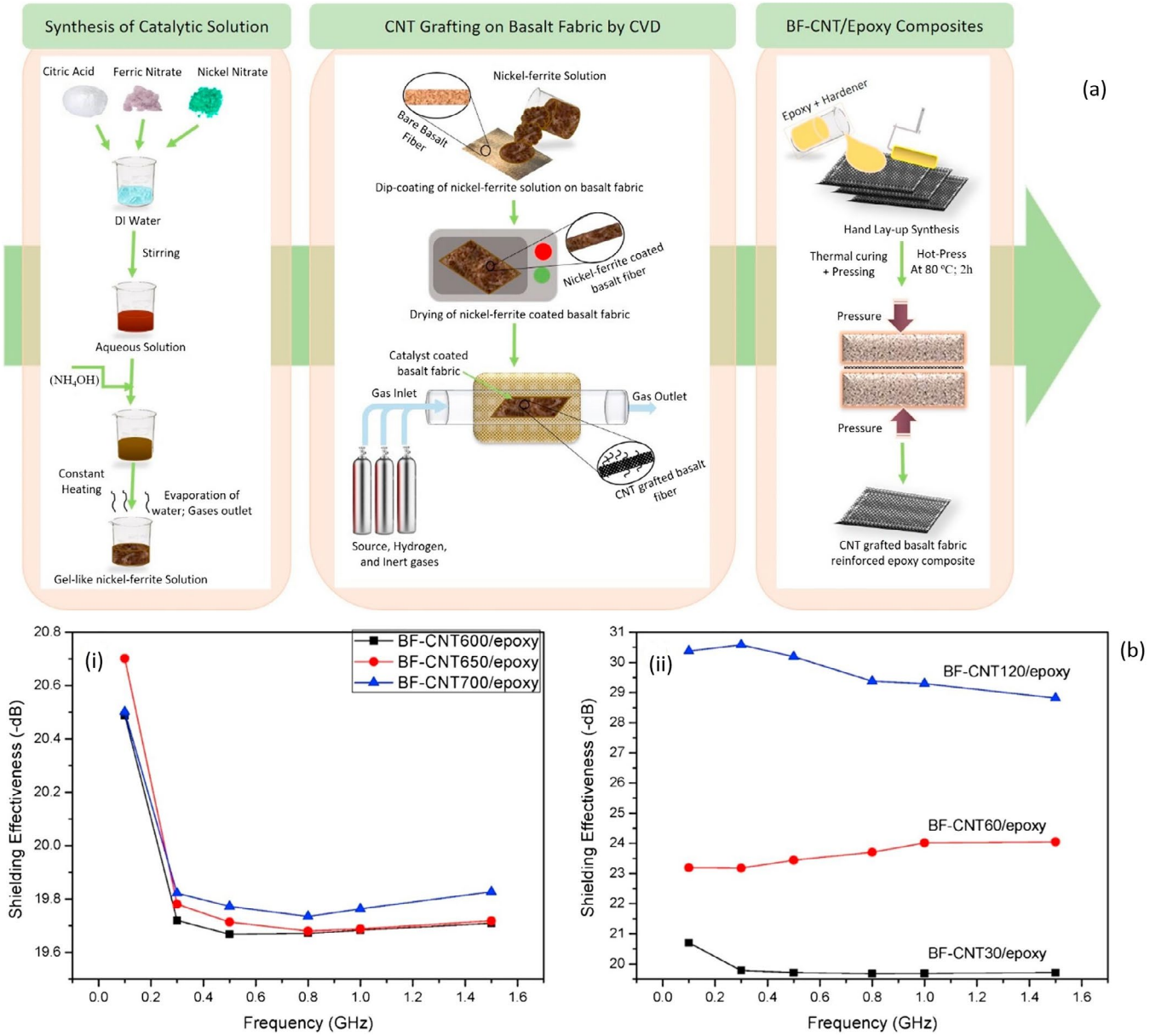

FIGURE 6 | (a) Schematic representation of the fabrication of the CNT-grafted basalt fabric reinforced epoxy composite. (b) Comparison of EMI shielding effectiveness of (i) BF-CNT600/epoxy, BF-CNT650/epoxy, and BF-CNT700/epoxy and (ii) BF-CNT30/epoxy, BF-CNT60/epoxy, and BF-CNT120/epoxy. *Source:* Adapted with permission [39]. Copyright 2018, Elsevier.

prepared grafted BF-CNT epoxy composites with CNT-reinforced epoxy/basalt fiber composites. In this study, the CNT-reinforced epoxy/basalt fiber composites were processed by dissolving samples in acetone, followed by 15 min of sonication. The samples were then dipped in epoxy resin, and the remaining acetone was evaporated by heating the solution to 60°C for 1.5 h. A hardener was added in a 2:1 ratio to the resin, and the samples were sandwiched with three plies of basalt fiber (BF) and CNT-reinforced epoxy resin using the hand-layup method. This assembly was then pressed at 80°C for 2 h. The samples were categorized by their weight percentages (wt%): 0.1, 0.5, and 1.0 wt%. These were compared to a pure BF sample, a BF-CNT/epoxy sample, and a BF-CNT sample grafted at 600°C for 30 min, excluding other samples from the previous study by Mittal et al. [39] that focused on varying deposition times and temperatures. The results, indicated that the EMI shielding efficiency (EMI SE) values were slightly improved for the BF-CNT/epoxy composite samples due to the inherent conductivity of the reinforced CNTs. Additionally, the BF-CNT epoxy samples exhibited a more uniform and continuous conductive network, which negatively affected the volume resistivity, as the conductivity of the shielding material is a crucial factor in determining EMI SE [132].

3.2 | Spray Drying

In the process of spray drying, a liquid feed is atomized into tiny droplets and combined with a heated gas stream, allowing the liquid to evaporate, and leaving behind only the dried-up solids. The solids are then removed from the gas stream and collected for later use as seen in Figure 7 [133].

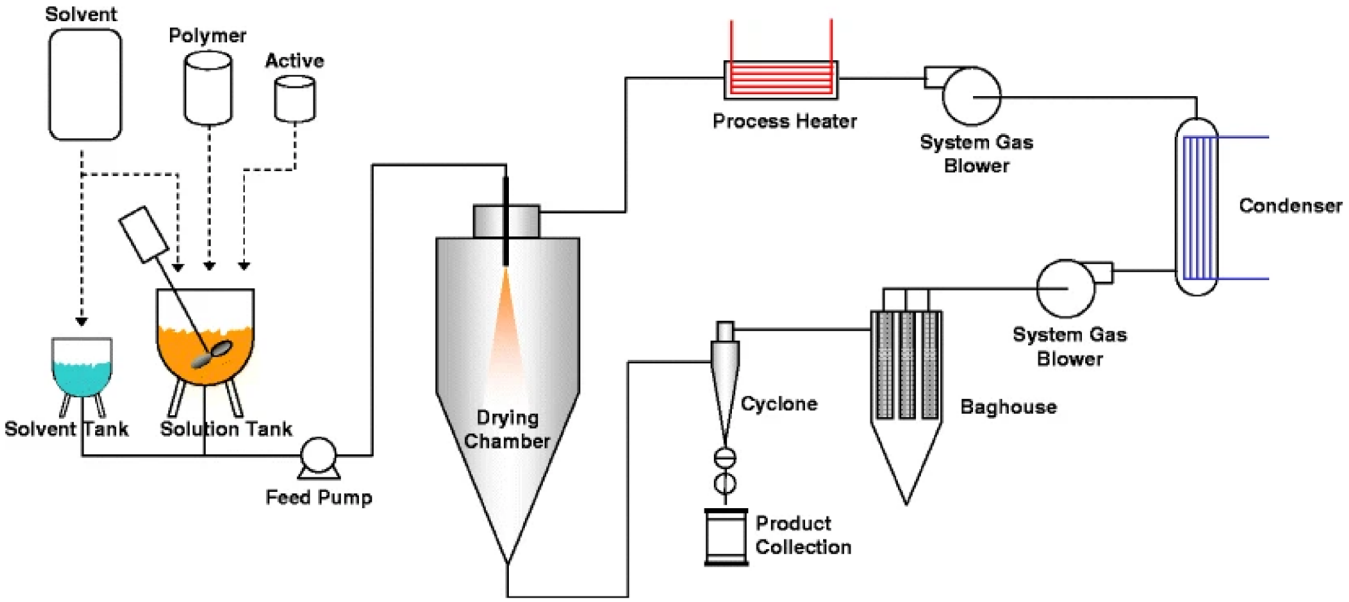

FIGURE 7 | Schematic representation of the spray drying process. *Source:* Reproduced with permission [133]. Copyright 2009, Springer.

Zhang et al. [134] investigated the effect of different treatment methods on the microwave absorption performance of Fe_3O_4, the initial material was synthesized via hydrothermal process to J. Liu method [135], then collected, washed and finally dried overnight, denoted as FE, a portion in addition to saccharose and suspension of CNTs was then treated with ultrasonic dispersion and then introduced to dry spraying, and for simplicity this sample was called FC. It was found the electromagnetic parameters of FC were greater than FE those being real parts of complex permittivity (ε′) and imaginary parts of complex permittivity (ε″), and as for the reflection loss, across the frequency range from 2 to 16, the reflection loss went from around 0 dB for FE to around −10 dB for FC at the frequencies of 10 to 12 Hz. The dielectric and magnetic loss tangents have also increased at increasing frequencies for the magnetic loss tangent and the opposite for dielectric loss tangent, over all the effect of spray drying has increased the microwave absorbance performance.

3.3 | Coating

The coating Table 2 summarizes the filler materials, the post-treatment methods used, along with EMI SE values at their respective operating frequencies, from recent literature to highlight the current research conducted for BFRPs in the context of EMI shielding process is a category of different methods that involve inserting the substrate in a solution of the desired material to be formed. Dip-drying [136], spin coating [137], impregnation [138] and spraying [139]. For basalt fiber composites, the most common method is the dip-drying method, which involves dipping the substrate in an aqueous solution containing the desired material for a period of time, and then drying the sample in an oven over a period of time. This coating process is favorable over others because of its simplicity, lack of chemical reactions, adding no chemical solvents, and the possibility of a higher number of fillers on the substrate [140–143].

As shown in Figure 8a, Kim et al. [136] fabricated the MWCNT-coated basalt fiber composites by dilution of MWCNT/SDS (Sodium dodecyl sulfate) dispersion with distilled water to produce an aqueous dispersion with 0.5 wt% MWCNT. The BFs were then dipped into the coating at ambient temperature for 1 min and dried in an oven with 120°C for 15 min. This process was repeated at cycles of 1, 2, 3, 5, and 10 which were used to denote the sample as BF-Cx, x being the number of cycles in the process. The MWCNT-coated basalt fiber/epoxy composites were then prepared by a hand lay-up method where 25 phr of DDM (4,4′-Diaminodiphenylmethane) was added to DGEBA (Diglycidyl ether of bisphenol A) and stirred at 80°C to produce a homogenous mixture. The MWCNT-coated basalt fibers were then impregnated with epoxy resin after which 3 plies of the fibers were stacked and hot-pressed at 150°C at a pressure of 150 MPa for 1 h. The final samples were denoted by BF-Cx/EP, x being the number of cycles in the process, and can be denoted for 0, 3, and 10 cycles in Figure 8b.

4 | Factors Affecting EMI Shielding Properties of the Filler Material

Basalt fibers have been a forerunner for EMI shielding materials due to favorable mechanical and thermal properties, simple processing techniques and environment-friendly manufacturing methods. Further looking into the factors that determine the above advantages, the conductive filler layer is examined by the thickness (number of layers), percentage by weight (wt%), conductivity, interfacial relationship, and the permeability. Therefore, when identifying a material that can be used as a conductive filler for BFs these factors have to be considered.

4.1 | Percentage by Weight

In BF composites, the percentage by weight, wt%, is one of the main factors that influenced the EMI shielding property. The

TABLE 2 | Summary of recent literature on BFRPs, their post-treatment methods and EMI SE values.

Filler materials	Post-treatment method	EMI shielding (dB) @ Operating frequency (GHz)	References
Graphite and Ag-coated Cu powders	Coated-finishing method	> 20 @ 0.01–3	[10]
Graphite, graphene	Double layer coating	72.9 @ 0–0.04	[37]
Co-Ni alloy-coated	Writing–grafting–activation–deposition	72.33 @ 8.2–12.4 (X band)	[38]
Carbon nanotubes	Chemical vapor deposition	30.38 @ 0.1	[39]
Carbon nanotubes/ Polydimethylsiloxane (PDMS)	Chemical vapor deposition	40.1 @ 8.2 (X band)	[109]
Carbon nanotubes/ Polydimethylsiloxane (PDMS)	Chemical vapor deposition	60 @ 8.2–12.4 (X band)	[110]
Aramid nanofibers/multiwalled carbon nanotubes	Vacuum-assisted filtration	24.6 @ 8.2–12.4 (X band)	[111]
Laser-induced graphene/epoxy resin	Hot-press curing/ Vacuum bagging	50 @ 8.2–12.4 (X band)	[114]
Cu-plated	Electroless plating	57 @ 0.03	[117]
Ni-plated		39 @ 0.03	
Cu and Ni-plated		65 @ 0.03	
Copper and Nickel-Cobalt alloy-plated		50 @ 0.03	
Multiwalled carbon nanotubes/ Ethylene methyl acrylate	Solution casting/ compression molding	20 @ 8.2–12.4 (X band)	[118]
Multiwalled carbon nanotubes/ polyvinyl alchohol	Electrospinning	31.5 @ 12	[120]
$Ti_3C_2T_x$	Facile spray-drying	41.53 @ 8.2–12.4 (X band)	[144]
Graphene/polyurethane	Double-layer coating	60 @ 0.01	[149]
Eutectic-Bi-Sn-coated/Carbon nanotubes/epoxy	Vacuum-assisted resin transfer method	30.4 @ 8.2–12.4 (X band)	[150]
Carbon nanotubes/ Polydimethylsiloxane	Chemical vapor deposition	37.37 @ 8.2–12.4 (X band)	[110]
Vanillin, glycerol triglycidyl ether, 1,10-diaminodecane, poly(vinyl alcohol-g-3,4-dihydroxybenzyl acetal), carbon nanotubes/graphene	Dip-coating	30.4 @ 8.2–12.4 (X band)	[112]
Single-walled carbon nanotubes	Sonication	81 @ 12	[151]

wt% indicates the content of the filler material used and is important to understand the behavior of the reflection, absorption and transmittance of the EMWs, and to optimize the material accordingly. Liu et al. [37] examined the electromagnetic properties of graphite and graphene-coated basalt fiber fabrics. The graphite wt% was changed for each sample and the graphene content was kept constant, and vice versa. The shielding efficiency was the same for the samples with minor differences as the graphite and graphene content increased. However, optimal wt% ranges were identified, beyond which excessive filler content could lead to detrimental effects such as aggregation or clustering, potentially compromising mechanical properties. This highlights the importance of precise wt% optimization to strike a balance between EMI shielding effectiveness and mechanical integrity in BF composites.

4.2 | Number of Layers

Thickness or the number of layers affects the EMW behavior in terms of dissipation because as the depth increases, the lesser the energy of the EMW. Therefore, in the same study by Chang et al. [109] mentioned before, the influence of thickness or the number of layers on the electromagnetic interference (EMI) properties of basalt fiber and carbon nanotubes (CNTs) nanocomposites was investigated. The study utilized BFF-CNT/PDMS

(Polydimethylsilioxane) samples, where PDMS acted as a matrix agent enhancing physical and chemical properties. It was observed that in BFF-CNT/PDMS composites, the shielding efficiency increased with the number of layers (thickness), as depicted in Figure 9. Similarly, Liu et al. [37] examined the impact of thickness on shielding efficiency in double-layer coated basalt fiber fabric with variations in graphite and graphene coating thickness. Results indicated that samples with thicker coatings exhibited higher shielding efficiency. This correlation highlights the significance of thickness in influencing EMI properties and interfacial behavior within composite materials, underscoring the importance of optimizing thickness for effective EMI shielding performance while considering practical and economic constraints.

Moreover, as shown in Figure 10, the hydrogen (H_2) flow rate significantly affects CNT growth on basalt fiber fabric (BFF) during the chemical vapor deposition (CVD) process. H_2 acts as a reducing agent, aiding in catalyst activity and removing excess carbon atoms. In Figure 10a, the untreated BFF has a smooth surface, while Figure 10b–d show an increasing number of CNTs as the H_2 flow rate rises. At 77 sccm (Figure 10e), CNTs fully cover the fiber, forming a dense network. However, when the flow rate reaches 98 sccm (Figure 10f), CNT growth declines due to dilution of the C_2H_2 carbon source and reduced carbon absorption on the catalyst, highlighting the need for optimized H_2 levels.

4.3 | Permeability

Another major factor being the permeability, the mechanisms of which were looked into above, is also a major factor that affects the EMI shielding properties of a material. Yu et al. [144] investigated the natural rubber TNR ($Ti_3C_2T_x$) layer and pure natural rubber (NR) on BF fabrics and their effect on electromagnetic properties where it was found that the EMI SE value is 41.53 dB which is ideal for shielding applications. The permeability ($\mu = \mu' - j\mu''$) affects the dielectric constant which in turn affects the electromagnetic loss and induces a magnetic field due to the motion of charges [145]. Figure 11 shows that the μ'' goes to negative as the frequency reached 11.5 GHz, which indicates that magnetic energy is released out of the BF/TNR sample as there is motion of charges. The permeability affects the SE_R attenuation of the total SE_T as the motion of charge carriers interferes with the incident EMWs [146].

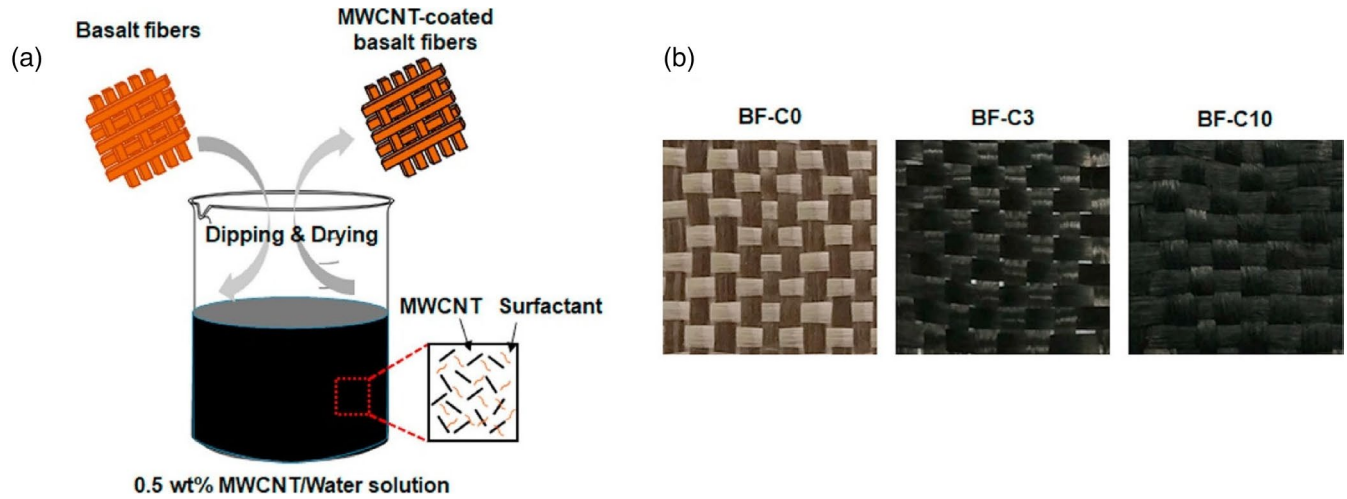

FIGURE 8 | (a) Schematic illustration of the dip-dry coating method for preparing MWCNT-coated basalt fibers (BF-Cx). (b) Digital images of MWCNT-coated basalt fibers with different dip-dry coating cycles. *Source:* Reproduced with permission [136]. Copyright 2019, Elsevier.

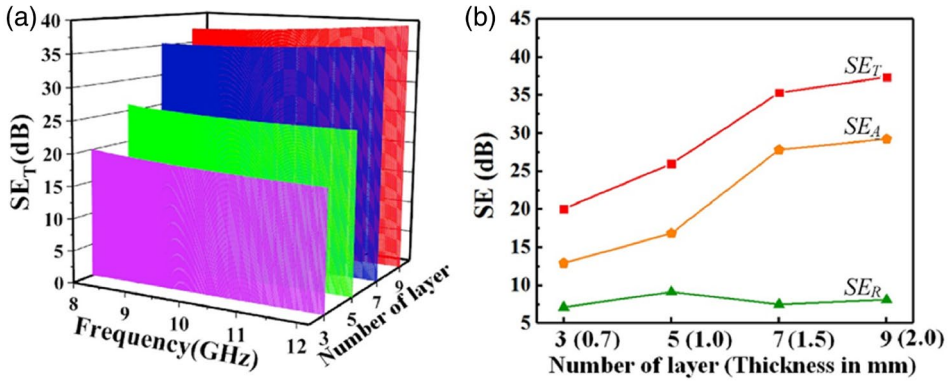

FIGURE 9 | EMI shielding against frequency and number of layers for BFF-CNT/PDMS. *Source:* Reproduced with permission [109]. Copyright 2020, Elsevier [144].

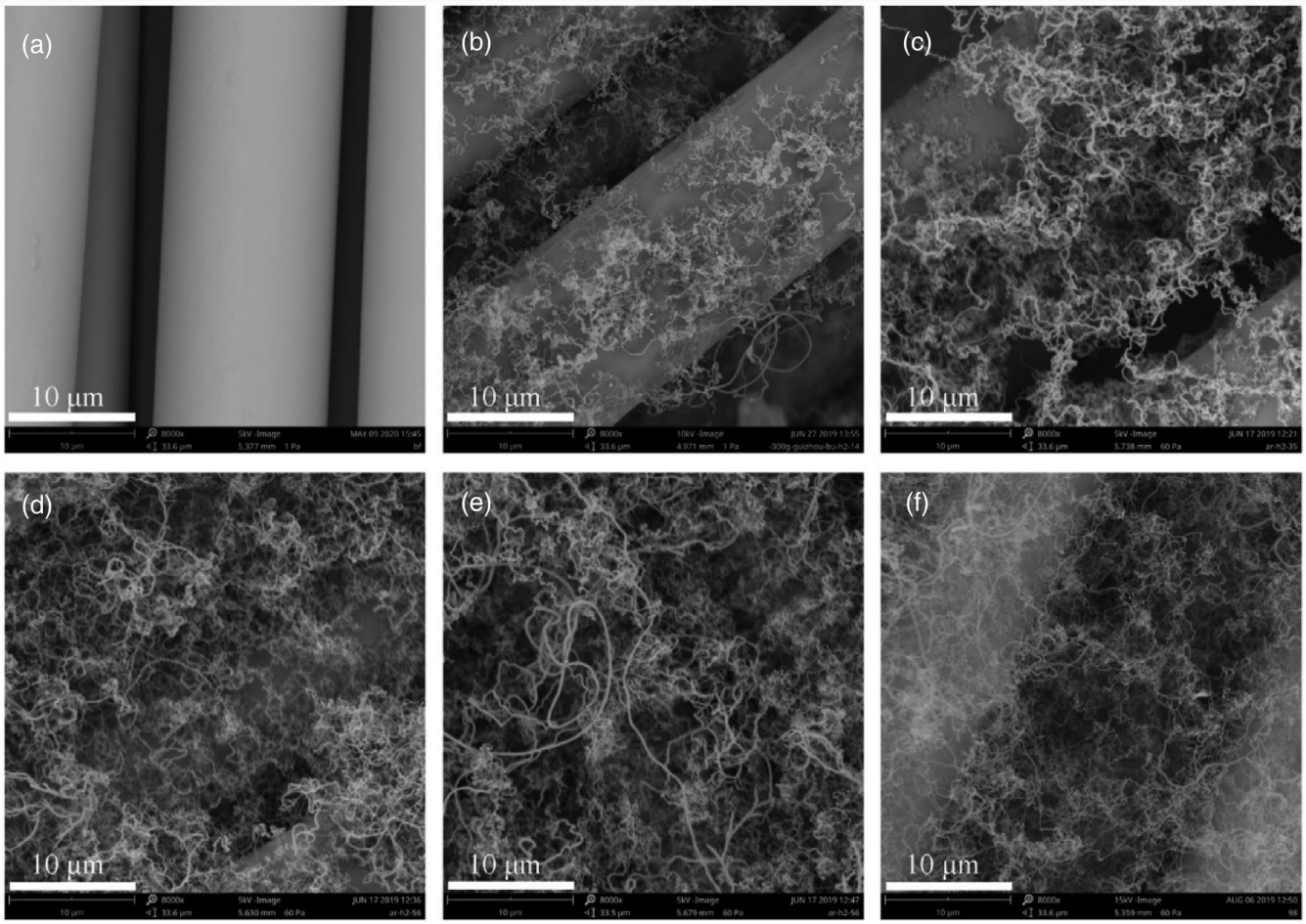

FIGURE 10 | SEM characterization of the basalt fiber carbon nanotube (BFF-CNT) samples with respect to hydrogen (H_2) flow rates (a) BFF; (b) BFF-CNT14; (c) BFF-CNT35; (d) BFF-CNT56; (e) BFF-CNT77; (f) BFF-CNT98. *Source:* Reproduced with permission [109]. Copyright 2020, Elsevier.

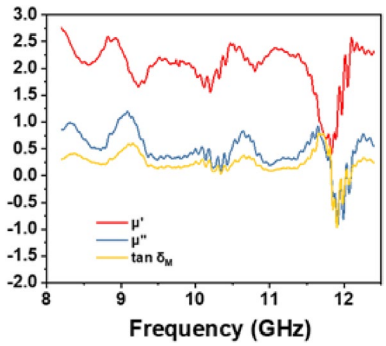

FIGURE 11 | Plots of real part of permeability (μ'), imaginary part of permeability (μ'') and tan δM of BF/T0/TNR fabric. *Source:* Reproduced with permission [144]. Copyright 2021, Elsevier.

4.4 | Conductivity

BFs are insulators thereby enabling the need for a conductive filler to be added and have a higher average SE value (25.89 dB) than the industry standard—20 dB [147]. This improves the conductivity of the material and can potentially increase the EMI SE of the entire material. The material has the advantage of benefitting from higher conductivity because the EMW gets reflected due to the larger presence of delocalized electrons, which can lead to increase of absorption, and the permeability, if high, can lead to a higher magnetization which in turn results in an increased magnetic loss [121, 123]. Moreover, in a study by Chen et al. [38], the conductivity of Co-Ni alloy-coated basalt fiber (BF) fabrics, determined by the deposition time of the coating, played a pivotal role in influencing their electromagnetic interference (EMI) properties. As conductivity increased with longer deposition times, ranging from 2.56 to 38.04 S cm^{-1}, a corresponding enhancement in EMI shielding effectiveness (SE) was observed, with SE values rising from 36.12 to 72.33 dB. Moreover, in the same study by Kim et al. [136], it can be seen that the conductivity directly affects the EMI SE of a material in Figure 12 which shows an increase in the electrical conductivity and decrease in the resistivity of the sample. The EMI results indicated that the treatment method significantly enhanced the electrical conductivity and reduced the resistivity of the MWCNT-coated basalt fiber/epoxy composites, thereby improving their EMI shielding efficiency (EMI SE) and other electromagnetic properties. Therefore, this correlation between conductivity and EMI SE underscores the significance of electrical conductivity in determining the material's ability to attenuate electromagnetic waves (EMWs). Higher conductivity facilitates better dissipation and reflection of EMWs within the material, resulting in improved shielding efficiency. Therefore, optimizing

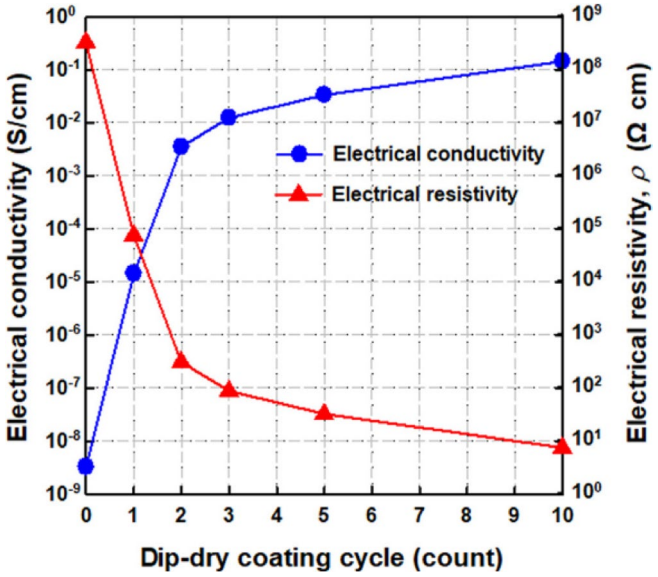

FIGURE 12 | Electrical conductivity and resistivity in the in-plane direction of the epoxy composites including MWCNT-coated basalt fibers with different dip-dry coating cycles. *Source:* Reproduced with permission [136]. Copyright 2019, Elsevier.

the conductivity of Co-Ni alloy-coated BF fabrics, achieved through careful control of deposition parameters like time, offers a promising avenue for enhancing their performance in EMI shielding applications.

4.5 | Interfacial Interaction

As covered in multiple literature above, interfacial interactions between the matrix and filler material affect the shielding efficiency, especially the SE_M attenuation. Due to the filler material's variable effects, the interfacial interaction between the fibers and the filler can favorably cause dissipation of the EMWs due to the dielectric loss. However, the EMW can potentially leave and this should be accounted for by more coatings or number of layers of the filler material, where the EMW is shielded by the reflection and absorption of the subsequent layer [148]. Moreover, the BF that are further inside, coupled with the network of the filler material, can aid in multiple reflections which further increases the attenuations SE_A and SE_R (Table 2).

5 | Applications and Future Perspectives

Given the recent years of advancement in all technological areas, there is more exposure to electromagnetic interference and waves to both humans and electronic equipment which warrants the need to advance electromagnetic interference shielding technologies furthermore. For example, real-time detection machines and monitoring systems can suffer from interference, such as radars, air traffic control and weather control, under the effect of damage monitoring tools are more exposed to electromagnetic waves.

Electromagnetic shielding technology is crucial in military campaigns as well to safeguard military equipment from jamming attacks and interferences, Lin et al. [114] provided a facile approach to fabricate multi-functional basalt fiber reinforced epoxy composites with high ballistic impact resistance and electromagnetic interference shielding properties, making it very suitable for the defense industries. Zhao et al. [112], achieved a biobased, recyclable, and multi-functional high performance basalt fiber-based composite which is deemed appropriate for both military and commercial use given it meets the required shielding performances of 30 and 20 dB, respectively for both domains, the material boasts superior thermal and mechanical properties, exhibiting self-adhesion behaviors making a perfect candidate for such applications. Finally, as previously mentioned, Lin et al. [114] stresses its importance in the medical sector as electromagnetic radiation is used in all MRI activities which interferes with the normal operation of the equipment as well as doctors and technicians and other staff members, as well as ensure the functionality of life-sustaining devices like pacemakers and cochlear implants by preventing interference from external electronic devices.

Since EMI shielding is becoming an urgent industry application, more research is being conducted to identify, improve and optimize materials that can aid in the application. As mentioned above, basalt fiber composites have been chosen as an eco-friendly, economic, and abundant alternative to carbon-based fiber composites, metal composites and polymer-based composites for EMI shielding. Moreover, the mechanical and chemical properties make basalt fibers ideal for the application of EMI shielding. However, since basalt fiber is an insulator, a conductive filler needs to be used to accommodate for the conductivity since EMI shielding depends on conductivity, among other properties. Basalt fiber has a higher strength-to-cost ratio, non-toxic and good chemical resistance compared to carbon fibers. It has superior mechanical properties compared to glass fibers. Basalt fibers have large surface area and with nanofillers, the surface area can be improved which can improve EMI SE due to more multiple reflections. The interfacial area is also something that can be improved with a conductive filler, preferably a nanofiller as well. This can improve the electrical properties and the magnetic properties of the BF composite which can enhance the EMI SE. Moreover, the post treatment of basalt fiber composites allows for different filler materials to be used which can be used to improve the existing properties of basalt fibers.

The conductive fillers added improved dielectric properties due to dielectric loss and also the magnetic properties such as good permeability of the material overall which aided in improving the total EMI SE values of the composite. The post treatment methods such as chemical vapor deposition, spray-drying and coating were examined and the filler material showed improved EMI SE of the overall composite. The factors that affected the EMI SE such as the percentage by weight of the filler material, the conductivity, thickness, permeability and the interfacial interaction were investigated to show how these materials affected the EMI SE values.

Basalt fiber composites offer promising potential for electromagnetic interference (EMI) shielding applications. When considering EMI shielding effectiveness, several parameters play a crucial role in the design and optimization of basalt fiber composites.

- First, the choice of matrix material is significant. While basalt fibers possess intrinsic electrical insulating properties, incorporating a conductive matrix, such as a conductive polymer or metal-coated matrix, can enhance the EMI shielding performance.
- Second, the architecture and arrangement of basalt yarns in the fabric structure are essential. The use of conductive basalt yarns or the integration of conductive coatings on the yarns can improve the electrical conductivity of the composite, thus enhancing EMI shielding.
- Third, in multilayer composites, the layer architecture and the incorporation of additional shielding layers can further augment the shielding effectiveness. Finally, the orientation and distribution of basalt fibers within the composite play a crucial role. Optimizing fiber alignment and distribution to ensure efficient electromagnetic wave absorption and reflection can significantly enhance EMI shielding.

Therefore, in terms of improvements, further research can focus on developing advanced conductive matrix materials specifically tailored for basalt fiber composites, optimizing the arrangement and density of conductive yarns, exploring further interfacial interactions between matrix and reinforced material, and investigating innovative fiber alignment techniques to maximize EMI shielding performance.

- The use of electromagnetic shielding basalt fiber composites can aid in the creation of radars. These composites can efficiently lessen electromagnetic interference, improving the efficiency and precision of radar. Basalt fiber composites are appropriate for radar system components due to their lightweight and robustness, which enables the development of effective and dependable radar systems.
- Using advanced conductive matrix materials to improve conductivity enhances electromagnetic shielding efficiency. Carbon nanotubes (CNTs) and metal nanoparticles have gained significant attention, but other conductive materials show promise too. Conductive polymers like polyaniline and poly(3,4-ethylenedioxythiophene) (PEDOT) can serve as matrix materials, providing high electrical conductivity while being lightweight and formable [152]. Metal coatings on basalt fibers, such as copper, silver, or nickel, enhance electrical conductivity and contribute to effective EMI shielding. Conductive nanocomposites combine basalt fibers with conductive fillers like carbon black, carbon fibers, or conductive ceramics, resulting in improved EMI shielding. MXenes, 2D transition metal carbides, nitrides, or carbonitrides, are emerging options that can be incorporated into the composite matrix or applied as coatings on basalt fibers, significantly enhancing electrical conductivity and EMI shielding effectiveness [153, 154]. These materials offer opportunities to tailor EMI shielding properties in basalt fiber composites, with potential applications in diverse fields. Further research is needed to optimize their dispersion, concentration, and integration within the composite structure to maximize EMI shielding effectiveness.
- Studying the interfacial interactions in basalt fiber composites is crucial for determining their electromagnetic interference (EMI) shielding capabilities. The morphology, adhesion, chemical interactions, and bonding at the fiber-matrix interface directly affect the composite's electrical conductivity and EMI shielding performance. Mechanical testing methods offer quantitative data on interfacial strength and adhesion, ensuring the integrity and stability of conductive pathways, leading to enhanced EMI shielding. Computational modeling and simulations complement experimental investigations by providing a deeper understanding of the interfacial behavior at the atomic level. By correlating interfacial interactions with EMI shielding capabilities, researchers can identify key factors for optimal shielding performance, guiding the development of basalt fiber composites with enhanced EMI shielding for various industries.
- Optimizing the arrangement and density of the conductive layer in basalt fiber composites is crucial for effective electromagnetic interference (EMI) shielding. Achieving continuous and uniform coverage throughout the composite minimizes gaps or voids that can compromise shielding performance. Techniques such as electrostatic deposition or chemical vapor deposition achieve a uniform arrangement. The density of the conductive layer should balance creating sufficient conductive pathways for efficient charge transfer and avoiding excessive weight and reduced flexibility. Multilayer composites with different materials or thicknesses can enhance EMI shielding through impedance mismatch, reflection, and absorption. Experimental techniques like impedance measurements and shielding effectiveness tests, along with numerical simulations, support optimization efforts. By optimizing the arrangement and density of the conductive layer, basalt fiber composites achieve efficient coverage, enhanced charge transfer, and improved EMI shielding effectiveness while considering other functional requirements such as weight and flexibility. Moreover, finite element analysis (FEA) software allows for parameter optimization through simulations, reducing experimental costs and time. Exploring new fiber alignment techniques, such as oriented alignment, electrospinning/electrostatic alignment, magnetic field alignment, and additive manufacturing, can strengthen basalt fibers in composites and maximize EMI shielding efficiency [155–157]. By achieving better fiber alignment, these techniques enhance the mechanical properties of the composite and improve its EMI shielding performance.
- In many disciplines, electrospinning technology has made significant advancements. The specialized research on electrospinning for use in EMI shielding is still in the early stages of development, highlighting the necessity for additional work to attain practical applications. Despite ongoing research, obstacles remain that must be overcome to realize the commercialization of promising electrospun-based EMI shielding composites.
- Future advancements in electromagnetic interference (EMI) shielding using basalt fiber-reinforced polymer (BFRP) composites could benefit significantly from the integration of metamaterials and Frequency Selective Surfaces (FSS). Metamaterials, known for their capacity to manipulate electromagnetic wave propagation [158], offer a transformative

approach to enhancing the shielding capabilities of BFRPs. By incorporating metamaterials, it becomes possible to tailor the behavior of electromagnetic waves within the composite, optimizing shielding efficiency across various frequency ranges. Concurrently, FSS, which are engineered to selectively transmit or block specific frequencies [159], could work synergistically with metamaterials to further enhance the targeted shielding capabilities of BFRPs. Such innovations are particularly relevant to applications in telecommunications, aerospace, and military systems, where precise frequency control is critical. Future research should focus on the development of lightweight, scalable designs that integrate the mechanical robustness of basalt fibers with the advanced electromagnetic manipulation properties of metamaterials and FSS, thereby achieving superior shielding performance.

- An emerging research focus within EMI shielding materials is the development of absorption-dominated materials that minimize electromagnetic wave reflection while maximizing absorption. This approach not only enhances shielding effectiveness by reducing interference but also aligns with increasing sustainability goals in materials science. Basalt fiber-reinforced polymers (BFRPs), when combined with eco-friendly fillers and conductive coatings, represent a promising avenue for the development of green EMI shielding solutions. These composites can be engineered to exhibit high absorption rates, thus contributing to effective shielding while minimizing their environmental footprint [160, 161]. Moreover, the ability to tune the electromagnetic response of these composites to specific frequency bands offers considerable potential for their use in industries such as renewable energy, smart cities, and environmental monitoring [162]. Future research directions could explore optimizing the tunability of these materials to meet the specific performance demands of various applications, further advancing the role of BFRPs in sustainable technology development.

6 | Conclusion

Basalt fiber composites with electromagnetic shielding have a lot of potential in the future. First off, it is anticipated that limitations on commercialization would lessen as the technology develops and receives regulatory approval. These composites could meet industry requirements and broaden their market reach with improvements in manufacturing procedures and material optimization. Basalt fiber composites have great promise for EMI shielding in challenging situations. Basalt fibers are perfect for applications requiring resistance to extreme temperatures and corrosion because of their inherent qualities of high strength, corrosion resistance, and thermal stability. These materials' improved electromagnetic shielding properties help protect delicate electronics and equipment in sectors like aerospace, defense, and offshore energy. Continued research and development activities are projected to lower the overall costs related to manufacturing basalt fiber composites, which will reduce their commercialization costs. Economies of scale and improved production techniques will help to lower costs as the need for electromagnetic shielding solutions rises, making the technology more available and cheaper for a variety of industries. Finally, with improvements in commercialization, EMI shielding in challenging conditions, cost reduction, and radar development likely to contribute to their widespread usage across different industries, the future prospects of electromagnetic shielding basalt fiber composites appear positive overall.

Conflicts of Interest

The authors declare no conflicts of interest.

References

1. J.-M. Thomassin, C. Jérôme, T. Pardoen, C. Bailly, I. Huynen, and C. Detrembleur, "Polymer/Carbon Based Composites as Electromagnetic Interference (EMI) Shielding Materials," *Materials Science and Engineering: R: Reports* 74 (2013): 211–232.

2. W. A. Radasky and M. Bäckström, "Brief Historical Review and Bibliography for Intentional Electromagnetic Interference (IEMI)," in *2014 XXXIth URSI General Assembly and Scientific Symposium* (*URSI GASS*) (IEEE, 2014), 1–4.

3. W. A. Radasky, "The Role of Electromagnetic Shielding in Dealing With the Threat of Intentional Electromagnetic Interference (IEMI)," in *2015 International Conference on Electromagnetics in Advanced Applications* (*ICEAA*) (IEEE, 2015), 1145–1148.

4. A. Sirswal and M. K. Dewan, "Modeling Effect of Electromagnetic Interference on Cardiovascular System," *International Journal for Research in Applied Science and Engineering Technology* 9 (2016): 1–7.

5. R. G. Olsen, S. D. Schennum, and V. L. Chartier, "Comparison of Several Methods for Calculating Power Line Electromagnetic Interference Levels and Calibration With Long Term Data," *IEEE Transactions on Power Delivery* 7 (1992): 903–913.

6. M. Jaroszewski, S. Thomas, and A. V. Rane, *Advanced Materials for Electromagnetic Shielding: Fundamentals, Properties, and Applications* (Hoboken, NJ: Wiley, 2018).

7. X. C. Tong, *Advanced Materials and Design for Electromagnetic Interference Shielding* (Boca Raton, FL: CRC Press, 2016).

8. G. Ma, J. Sun, L. Wang, F. Aslani, and M. Liu, "Electromagnetic and Microwave Absorbing Properties of Cementitious Composite for 3D Printing Containing Waste Copper Solids," *Cement and Concrete Composites* 94 (2018): 215–225.

9. Z. Zeng, F. Jiang, Y. Yue, et al., "Flexible and Ultrathin Waterproof Cellular Membranes Based on High-Conjunction Metal-Wrapped Polymer Nanofibers for Electromagnetic Interference Shielding," *Advanced Materials* 32 (2020): 1908496.

10. Y. Liu, Y. Yu, and X. Zhao, "The Influence of the Ratio of Graphite to Silver-Coated Copper Powders on the Electromagnetic and Mechanical Properties of Single-Layer Coated Composites," *Journal of the Textile Institute* 112 (2021): 1709–1716.

11. H.-R. Kim, K. Fujimori, B.-S. Kim, and I.-S. Kim, "Lightweight Nanofibrous EMI Shielding Nanowebs Prepared by Electrospinning and Metallization," *Composites Science and Technology* 72 (2012): 1233–1239.

12. T. Blachowicz, A. Hütten, and A. Ehrmann, "Electromagnetic Interference Shielding With Electrospun Nanofiber Mats—A Review of Production, Physical Properties and Performance," *Fibers* 10 (2022): 47.

13. N. Zhang, R. Zhao, D. He, et al., "Lightweight and Flexible Ni-Co Alloy Nanoparticle-Coated Electrospun Polymer Nanofiber Hybrid Membranes for High-Performance Electromagnetic Interference Shielding," *Journal of Alloys and Compounds* 784 (2019): 244–255.

14. X. Luo and D. D. L. Chung, "Electromagnetic Interference Shielding Using Continuous Carbon-Fiber Carbon-Matrix and Polymer-Matrix Composites," *Composites Part B: Engineering* 30 (1999): 227–231.

15. A. Ameli, P. U. Jung, and C. B. Park, "Electrical Properties and Electromagnetic Interference Shielding Effectiveness of Polypropylene/Carbon Fiber Composite Foams," *Carbon N Y* 60 (2013): 379–391.

16. J. Wu and D. D. L. Chung, "Increasing the Electromagnetic Interference Shielding Effectiveness of Carbon Fiber Polymer–Matrix Composite by Using Activated Carbon Fibers," *Carbon N Y* 40 (2002): 445–447.

17. S.-S. Tzeng and F.-Y. Chang, "EMI Shielding Effectiveness of Metal-Coated Carbon Fiber-Reinforced ABS Composites," *Materials Science and Engineering A* 302 (2001): 258–267.

18. M. Li, K. Yang, W. Zhu, et al., "Copper-Coated Reduced Graphene Oxide Fiber Mesh-Polymer Composite Films for Electromagnetic Interference Shielding," *ACS Applied Nano Materials* 3 (2020): 5565–5574.

19. A. Darvishzadeh and K. Nasouri, "Structural Engineering of Nickel-Coated Carbon Fibers With High Electrical Conductivity for Flexible EMI Shielding," *Journal of Materials Science: Materials in Electronics* 33 (2022): 5648–5660.

20. S. H. Lee, J. Y. Kim, C. M. Koo, and W. N. Kim, "Effects of Processing Methods on the Electrical Conductivity, Electromagnetic Parameters, and EMI Shielding Effectiveness of Polypropylene/Nickel-Coated Carbon Fiber Composites," *Macromolecular Research* 25 (2017): 936–943.

21. F. Fang, Y.-Q. Li, H.-M. Xiao, N. Hu, and S.-Y. Fu, "Layer-Structured Silver Nanowire/Polyaniline Composite Film as a High Performance X-Band EMI Shielding Material," *Journal of Materials Chemistry C* 4 (2016): 4193–4203.

22. M. Wang, X.-H. Tang, J.-H. Cai, H. Wu, J.-B. Shen, and S.-Y. Guo, "Construction, Mechanism and Prospective of Conductive Polymer Composites With Multiple Interfaces for Electromagnetic Interference Shielding: A Review," *Carbon N Y* 177 (2021): 377–402.

23. N. F. Colaneri and L. W. Schacklette, "EMI Shielding Measurements of Conductive Polymer Blends," *IEEE Transactions on Instrumentation and Measurement* 41 (1992): 291–297.

24. P. S. Liu, H. B. Qing, H. L. Hou, Y. Q. Wang, and Y. L. Zhang, "EMI Shielding and Thermal Conductivity of a High Porosity Reticular Titanium Foam," *Materials and Design* 92 (2016): 823–828.

25. H. Gao, C. Wang, Z. Yang, and Y. Zhang, "3D Porous Nickel Metal Foam/Polyaniline Heterostructure With Excellent Electromagnetic Interference Shielding Capability and Superior Absorption Based on Pre-Constructed Macroscopic Conductive Framework," *Composites Science and Technology* 213 (2021): 108896.

26. J. Joseph, A. Sharma, B. Sahoo, J. Paul, and A. M. Sidpara, "PVA/MLG/MWCNT Hybrid Composites for X Band EMI Shielding – Study of Mechanical, Electrical, Thermal and Tribological Properties," *Materials Today Communications* 23 (2020): 100941.

27. R. B. J. Chandra, B. Shivamurthy, S. D. Kulkarni, and M. S. Kumar, "Hybrid Polymer Composites for EMI Shielding Application – A Review," *Materials Research Express* 6 (2019): 082008.

28. C. H. Gireesh, K. Ramji, K. G. D. Prasad, and B. Srinu, "Study of Mechanical Properties and EMI Shielding Behaviour of Al6061 Hybrid Metal Matrix Composites," *International Journal of Surface Engineering and Interdisciplinary Materials Science (IJSEIMS)* 7 (2019): 48–63.

29. S. Budumuru and M. S. Anuradha, "Electromagnetic Shielding and Mechanical Properties of AL6061 Metal Matrix Composite at X-Band for Oblique Incidence," *Advanced Composites and Hybrid Materials* 4 (2021): 1113–1121.

30. D. C. Silveira, N. Gomes, M. C. Rezende, and E. C. Botelho, "Electromagnetic Properties of Multifunctional Composites Based on Glass Fiber Prepreg and Ni/Carbon Fiber Veil," *Journal of Aerospace Technology and Management* 9 (2017): 231–240.

31. S. Das and T. Yokozeki, "A Brief Review of Modified Conductive Carbon/Glass Fibre Reinforced Composites for Structural Applications: Lightning Strike Protection, Electromagnetic Shielding, and Strain Sensing," *Composites Part C: Open Access* 5 (2021): 100162.

32. F. Liu, Y. Gao, G. Wang, et al., "Laser-Induced Graphene Enabled Additive Manufacturing of Multifunctional 3D Architectures With Freeform Structures," *Advanced Science* 10 (2023): 2204990.

33. Z. Zeng, C. Wang, G. Siqueira, et al., "Nanocellulose-MXene Biomimetic Aerogels With Orientation-Tunable Electromagnetic Interference Shielding Performance," *Advanced Science* 7 (2020): 2000979.

34. L. Li, Y. Yan, J. Liang, et al., "Wearable EMI Shielding Composite Films With Integrated Optimization of Electrical Safety, Biosafety and Thermal Safety," *Advanced Science* 11 (2024): 2400887.

35. H. He, R. Zhang, P. Zhang, et al., "Functional Carbon From Nature: Biomass-Derived Carbon Materials and the Recent Progress of Their Applications," *Advanced Science* 10 (2023): 2205557.

36. H. Ye, Y. Wu, X. Jin, et al., "Creation of Wood-Based Hierarchical Superstructures via in Situ Growth of ZIF-8 for Enhancing Mechanical Strength and Electromagnetic Shielding Performance," *Advanced Science* 11 (2024): 2400074.

37. Y. Liu, Y. Yu, and H. Du, "The Influence of Two Types of Functional Particles on the Electromagnetic Properties and Mechanical Properties of Double-Layer Coated Basalt Fiber Fabrics," *Textile Research Journal* 92 (2021): 2591–2604.

38. C. Chen, Q. Yu, W. Hai, et al., "Flexible Sandwich-Structured Co–Ni Alloy-Coated Basalt Fabrics via the Writing–Grafting–Activation–Deposition Process for Electromagnetic Interference Shielding and Electrothermal Conversion," *ACS Applied Electronic Materials* 4 (2022): 6106–6116.

39. G. Mittal and K. Y. Rhee, "Hierarchical Structures of CNT@Basalt Fabric for Tribological and Electrical Applications: Impact of Growth Temperature and Time During Synthesis," *Composites. Part A, Applied Science and Manufacturing* 115 (2018): 8–21.

40. L. V. Toropina, G. G. Vasyuk, V. L. Kornyushina, V. M. Dyaglev, Y. M. Rassadin, and M. A. Makarushina, "New Cloth From Basalt Fibres," *Fibre Chemistry* 27 (1995): 67–68.

41. C. Chen, Y. Gu, S. Wang, Z. Zhang, M. Li, and Z. Zhang, "Fabrication and Characterization of Structural/Dielectric Three-Phase Composite: Continuous Basalt Fiber Reinforced Epoxy Resin Modified With Graphene Nanoplates," *Composites. Part A, Applied Science and Manufacturing* 94 (2017): 199–208.

42. S. G. Hu, K. Tian, and Q. J. Ding, "Design and Test of New Cement Based Microwave Absorbing Materials," in 2008 *8th International Symposium on Antennas, Propagation and EM Theory* (IEEE, 2008), 956–959.

43. J. Fořt, J. Kočí, and R. Černý, "Environmental Efficiency Aspects of Basalt Fibers Reinforcement in Concrete Mixtures," *Energies (Basel)* 14 (2021): 7736.

44. D. Paul, US Patent 1438428A 1922.

45. R. Fangueiro, *Fibrous and Composite Materials for Civil Engineering Applications* (Cambridge, UK: Elsevier, 2011).

46. V. Dhand, G. Mittal, K. Y. Rhee, S.-J. Park, and D. Hui, "A Short Review on Basalt Fiber Reinforced Polymer Composites," *Composites Part B: Engineering* 73 (2015): 166–180.

47. K. Pareek and P. Saha, "Basalt Fiber and Its Composites: An Overview," in *Proceedings of National Conference on Advances in Structural Technologies* (*CoAST-2019*) (Department of Civil Engineering National Institute of Technology Silchar, 2019), 3.

48. A. Saleem, L. Medina, M. Skrifvars, and L. Berglin, "Hybrid Polymer Composites of Bio-Based Bast Fibers With Glass, Carbon and Basalt Fibers for Automotive Applications—A Review," *Molecules* 25 (2020): 4933.

49. M. J. Le Bas and A. L. Streckeisen, "The IUGS Systematics of Igneous Rocks," *Journal of the Geological Society of London* 148 (1991): 825–833.

50. J. M. F. de Paiva, A. D. N. dos Santos, and M. C. Rezende, "Mechanical and Morphological Characterizations of Carbon Fiber Fabric Reinforced Epoxy Composites Used in Aeronautical Field," *Materials Research* 12 (2009): 367–374.

51. P. Chakartnarodom, W. Prakaypan, P. Ineure, N. Kongkajun, and N. Chuankrerkkul, "Feasibility Study of Using Basalt Fibers as the Reinforcement Phase in Fiber-Cement Products," *Key Engineering Materials* 766 (2018): 252–257.

52. H. Liu, Y. Yu, Y. Liu, et al., "A Review on Basalt Fiber Composites and Their Applications in Clean Energy Sector and Power Grids," *Polymers (Basel)* 14 (2022): 2376, https://doi.org/10.3390/polym14122376.

53. J. Sim and C. Park, "Characteristics of Basalt Fiber as a Strengthening Material for Concrete Structures," *Composites Part B: Engineering* 36 (2005): 504–512.

54. N. N. Morozov, V. S. Bakunov, E. N. Morozov, et al., "Materials Based on Basalts from the European North of Russia," *Glass and Ceramics* 58 (2001): 100–104.

55. A. G. Novitskii and M. V. Efremov, "Some Aspects of the Manufacturing Process for Obtaining Continuous Basalt Fiber," *Glass and Ceramics* 67 (2011): 361–365.

56. T. Czigány, "Discontinuous Basalt Fiber-Reinforced Hybrid Composites," in Polymer Composites, ed. K. Friedrich, S. Fakirov, and Z. Zhang (Boston: Springer, 2005), 309–328.

57. T. Czigány, "Basalt Fiber Reinforced Hybrid Polymer Composites," in *Materials Science Forum*, vol. 473-474 (Trans Tech Publications Ltd, 2005), 59–66.

58. H. Jamshaid and R. Mishra, "A Green Material From Rock: Basalt Fiber – A Review," *Journal of the Textile Institute* 107 (2016): 923–937.

59. H. Jamshaid, J. Militký, R. Mishra, and L. Koukolikova, "Basalt Fibers and Their Composites," *Novelties in Fibrous Material Science* (2017): 2.

60. H. Li, G. Xian, B. Xiao, and J. Wu, "Comprehensive Characterization of BFRP Applied in Civil Engineering," in *Advances in FRP Composites in Civil Engineering*, eds. L. Ye, P. Feng, and Q. Yue (Berlin, Heidelberg: Springer Berlin Heidelberg, 2011), 65–68.

61. V. Lopresto, C. Leone, and I. De Iorio, "Mechanical Characterisation of Basalt Fibre Reinforced Plastic," *Composites Part B: Engineering* 42 (2011): 717–723.

62. V. Manikandan, J. T. Winowlin Jappes, S. M. Suresh Kumar, and P. Amuthakkannan, "Investigation of the Effect of Surface Modifications on the Mechanical Properties of Basalt Fibre Reinforced Polymer Composites," *Composites Part B: Engineering* 43 (2012): 812–818.

63. G. Sezemanas, J. Keriene, M. Sinica, A. Lankaitis, and D. Mikulskis, "The Alkali and Temperature Resistance of Some Fibres." *Materials Science* (Medžiagotyra) 11 (2005): 29–35.

64. X. H. Liu, "Preface," *Shanxi Science and Technology* 29 (2014): 87–739.

65. K. Mazur, P. Jakubowska, P. Romańska, and S. Kuciel, "Green High Density Polyethylene (HDPE) Reinforced With Basalt Fiber and Agricultural Fillers for Technical Applications," *Composites Part B: Engineering* 202 (2020): 108399.

66. M. Khan, M. Cao, S. H. Chu, and M. Ali, "Properties of Hybrid Steel-Basalt Fiber Reinforced Concrete Exposed to Different Surrounding Conditions," *Construction and Building Materials* 322 (2022): 126340.

67. X. Zhao, X. Wang, Z. Wu, T. Keller, and A. P. Vassilopoulos, "Temperature Effect on Fatigue Behavior of Basalt Fiber-Reinforced Polymer Composites," *Polymer Composites* 40 (2019): 2273–2283.

68. K. Lou, X. Wu, P. Xiao, and C. Zhang, "Investigation on Fatigue Performance of Asphalt Mixture Reinforced by Basalt Fiber," *Materials* 14 (2021): 14, https://doi.org/10.3390/ma14195596.

69. A. Singh Gill, D. Visotsky, L. Mears, and J. D. Summers, "Cost Estimation Model for Polyacrylonitrile-Based Carbon Fiber Manufacturing Process," *Journal of Manufacturing Science and Engineering* 139 (2017): 041011.

70. J. Liu, M. Chen, J. Yang, and Z. Wu, "Study on Mechanical Properties of Basalt Fibers Superior to E-Glass Fibers," *Journal of Natural Fibers* 19 (2022): 882–894.

71. A. Pavlović, T. Donchev, D. Petkova, and N. Staletović, "Sustainability of Alternative Reinforcement for Concrete Structures: Life Cycle Assessment of Basalt FRP Bars," *Construction and Building Materials* 334 (2022): 127424.

72. N. Garg and S. Shrivastava, "Environmental and Economic Comparison of FRP Reinforcements and Steel Reinforcements in Concrete Beams Based on Design Strength Parameter," in *Proceedings of the UKIERI Concrete Congress, Jalandhar, India* (2019), 5–8.

73. M. Inman, E. R. Thorhallsson, and K. Azrague, "A Mechanical and Environmental Assessment and Comparison of Basalt Fibre Reinforced Polymer (BFRP) Rebar and Steel Rebar in Concrete Beams," *Energy Procedia* 111 (2017): 31–40.

74. J.-C. Huang, "EMI Shielding Plastics: A Review," *Advances in Polymer Technology* 14 (1995): 137–150.

75. B. D. Mottahed and S. Manoochehri, "A Review of Research in Materials, Modeling and Simulation, Design Factors, Testing, and Measurements Related to Electromagnetic Interference Shielding," *Polymer – Plastics Technology and Engineering* 34 (1995): 271–346.

76. D. D. L. Chung, "Electromagnetic Interference Shielding Effectiveness of Carbon Materials," *Carbon N Y* 39 (2001): 279–285.

77. H. Guo, Y. Chen, Y. Li, et al., "Electrospun Fibrous Materials and Their Applications for Electromagnetic Interference Shielding: A Review," *Composites. Part A, Applied Science and Manufacturing* 143 (2021): 106309.

78. D. E. Clark, D. C. Folz, and J. K. West, "Processing Materials With Microwave Energy," *Materials Science and Engineering A* 287 (2000): 153–158.

79. S. Gupta and N.-H. Tai, "Carbon Materials and Their Composites for Electromagnetic Interference Shielding Effectiveness in X-Band," *Carbon N Y* 152 (2019): 159–187.

80. J. Joo and A. J. Epstein, "Electromagnetic Radiation Shielding by Intrinsically Conducting Polymers," *Applied Physics Letters* 65 (1994): 2278–2280.

81. K.-H. Gonschorek and R. Vick, "Skin Effect and Shielding Theory of Schelkunoff," in *Electromagnetic Compatibility for Device Design and System Integration* (Berlin, Heidelberg: Springer, 2010), 377–392.

82. R. Ravindren, S. Mondal, K. Nath, and N. C. Das, "Investigation of Electrical Conductivity and Electromagnetic Interference Shielding Effectiveness of Preferentially Distributed Conductive Filler in Highly Flexible Polymer Blends Nanocomposites," *Composites. Part A, Applied Science and Manufacturing* 118 (2019): 75–89.

83. D. Wanasinghe and F. Aslani, "A Review on Recent Advancement of Electromagnetic Interference Shielding Novel Metallic Materials and Processes," *Composites Part B: Engineering* 176 (2019): 107207.

84. A. Joshi and S. Datar, "Carbon Nanostructure Composite for Electromagnetic Interference Shielding," *Pramana* 84 (2015): 1099–1116.

85. C. Chen and K. Naishadham, "Plane Wave Shielding Effectiveness of Conductive Polymer Films," in *IEEE Proceedings on Southeastcon*, vol. 1 (IEEE, 1990), 38–41.

86. Z. Liu, G. Bai, Y. Huang, et al., "Reflection and Absorption Contributions to the Electromagnetic Interference Shielding of Single-Walled Carbon Nanotube/Polyurethane Composites," *Carbon N Y* 45 (2007): 821–827.

87. S.-H. Lee, D. Kang, and I.-K. Oh, "Multilayered Graphene-Carbon Nanotube-Iron Oxide Three-Dimensional Heterostructure for Flexible Electromagnetic Interference Shielding Film," *Carbon N Y* 111 (2017): 248–257.

88. A. Chaudhary, R. Kumar, S. Teotia, S. K. Dhawan, S. R. Dhakate, and S. Kumari, "Integration of MCMBs/MWCNTs With Fe_3O_4 in a Flexible and Light Weight Composite Paper for Promising EMI Shielding Applications," *Journal of Materials Chemistry C* 5 (2017): 322–332.

89. A. Chaudhary, S. Kumari, R. Kumar, et al., "Lightweight and Easily Foldable MCMB-MWCNTs Composite Paper With Exceptional Electromagnetic Interference Shielding," *ACS Applied Materials and Interfaces* 8 (2016): 10600–10608.

90. J. Huo, L. Wang, and H. Yu, "Polymeric Nanocomposites for Electromagnetic Wave Absorption," *Journal of Materials Science* 44 (2009): 3917–3927.

91. S. B. Kondawar and P. R. Modak, "Theory of EMI Shielding," in *Materials for Potential EMI Shielding Applications*, eds. K. Joseph, R. Wilson, and G. George (Amsterdam: Elsevier, 2020), 9–25.

92. S. Das, A. K. Mukhopadhyay, S. Datta, and D. Basu, "Prospects of Microwave Processing: An Overview," *Bulletin of Materials Science* 32 (2009): 1–13.

93. H. C. Chen, K. C. Lee, J. H. Lin, and M. Koch, "Fabrication of Conductive Woven Fabric and Analysis of Electromagnetic Shielding via Measurement and Empirical Equation," *Journal of Materials Processing Technology* 184 (2007): 124–130.

94. A. K. Singh, A. Shishkin, T. Koppel, and N. Gupta, "A Review of Porous Lightweight Composite Materials for Electromagnetic Interference Shielding," *Composites Part B: Engineering* 149 (2018): 188–197.

95. Q. Li, Z. Zhang, L. Qi, Q. Liao, Z. Kang, and Y. Zhang, "Toward the Application of High Frequency Electromagnetic Wave Absorption by Carbon Nanostructures," *Advanced Science* 6 (2019): 1801057.

96. W. Deng, T. Li, H. Li, et al., "MOF Derivatives With Gradient Structure Anchored on Carbon Foam for High-Performance Electromagnetic Wave Absorption," *Small* 20 (2024): 2309806.

97. C. Jiang and B. Wen, "Construction of 1D Heterogeneous Co/C@ag Nws With Tunable Electromagnetic Wave Absorption and Shielding Performance," *Small* 19 (2023): 2301760.

98. A. Natan, N. Kuritz, and L. Kronik, "Polarizability, Susceptibility, and Dielectric Constant of Nanometer-Scale Molecular Films: A Microscopic View," *Advanced Functional Materials* 20 (2010): 2077–2084.

99. X. Zhang, J. Guo, P. Guan, G. Qin, and S. J. Pennycook, "Gigahertz Dielectric Polarization of Substitutional Single Niobium Atoms in Defective Graphitic Layers," *Physical Review Letters* 115 (2015): 147601.

100. A. A. Isari, A. Ghaffarkhah, S. A. Hashemi, S. Wuttke, and M. Arjmand, "Structural Design for EMI Shielding: From Underlying Mechanisms to Common Pitfalls," *Advanced Materials* 36 (2024): 2310683.

101. J. L. Violette, D. R. J. White, and M. F. Violette, "EMI Control in Analog and Digital Circuits," in *Electromagnetic Compatibility Handbook* (Dordrecht: Springer, 1987), 545–591.

102. H. C. Chen, K. C. Lee, J. H. Lin, and M. Koch, "Comparison of Electromagnetic Shielding Effectiveness Properties of Diverse Conductive Textiles via Various Measurement Techniques," *Journal of Materials Processing Technology* 192 (2007): 549–554.

103. D09 Committee n.d., https://doi.org/10.1520/d4935-18.

104. E. Håkansson, A. Amiet, and A. Kaynak, "Dielectric Characterization of Conducting Textiles Using Free Space Transmission Measurements: Accuracy and Methods for Improvement," *Synthetic Metals* 157 (2007): 1054–1063.

105. L. Y. Yeo and J. R. Friend, "Electrospinning Carbon Nanotube Polymer Composite Nanofibers," *Journal of Experimental Nanoscience* 1 (2006): 177–209.

106. B. Pant, M. Park, S.-J. Park, and H. Y. Kim, "High Strength Electrospun Nanofiber Mats via CNT Reinforcement: A Review," *Composites Research* 29 (2016): 186–193.

107. Y. Cai, T. Liu, L. Cheng, et al., "Superflexible Porous PCSnf-Fe_3O_4/CNT-PANI BP/PCSnf-Fe_3O_4 Sandwich Composite Films With Excellent Electromagnetic Wave Absorption Performance Based on Integral Assembly by Electrospinning," *Journal of Alloys and Compounds* 976 (2024): 173080.

108. R. Sharma, P. Benjwal, K. K. Kar, et al., "Carbon Nanotubes: Synthesis, Properties and Applications," in *Polymer Nano-Composites Based on Inorganic and Organic Nanomaterials* (Beverly, USA: Scrivener Publishing, 2015), 89.

109. C. Chang, X. Yue, B. Hao, D. Xing, and P.-C. Ma, "Direct Growth of Carbon Nanotubes on Basalt Fiber for the Application of Electromagnetic Interference Shielding," *Carbon N Y* 167 (2020): 31–39.

110. Z.-X. Chen, C. Chang, X. Yue, H. Li, C.-G. Liang, and P.-C. Ma, "Experimental and Theoretical Study on the Electromagnetic Shielding Performance of Polymer Nanocomposites Consisting of Basalt Fiber and CNTs," *Composites Science and Technology* 247 (2024): 110399.

111. S. Song, L. Li, D. Ji, J. Zhao, Q. Wu, and Q. Wang, "Flexible Basalt Fiber/Aramid Nanofiber/Carbon Nanotube Electromagnetic Shielding Paper With Outstanding Environmental Stability and Joule Heating Performance," *ACS Applied Materials and Interfaces* 15 (2023): 35495–35506.

112. X.-L. Zhao, Y.-D. Li, L.-Y. Zhan, and J.-B. Zeng, "Biobased, Recyclable, and Multi-Functional High-Performance Composites for Electromagnetic Interference Shielding," *Composites Science and Technology* 253 (2024): 110635.

113. T. Si, S. Xie, Z. Ji, et al., "In Situ Anchoring of Fe_3O_4/CNTs Hybrids on Basalt Fiber for Efficient Electromagnetic Wave Absorption," *Nanotechnology* 34 (2023): 405602.

114. G. Lin, T. Zhou, Z. Zhou, and W. Sun, "Laser Induced Graphene for EMI Shielding and Ballistic Impact Damage Detection in Basalt Fiber Reinforced Composites," *Composites Science and Technology* 242 (2023): 110182.

115. J. de la Roche, I. López-Cifuentes, and A. Jaramillo-Botero, "Influence of Lasing Parameters on the Morphology and Electrical Resistance of Polyimide-Based Laser-Induced Graphene (LIG)," *Carbon Letters* 33 (2023): 587–595.

116. T. Thaweeskulchai, K. Sakdaphetsiri, and A. Schulte, "Ten Years of Laser-Induced Graphene: Impact and Future Prospect on Biomedical, Healthcare, and Wearable Technology," *Microchimica Acta* 191 (2024): 292.

117. V. D. Skopintsev, T. D. Firsova, and E. G. Vinokurov, "Metal-Plated Carbon and Basalt Fabrics for Shielding of Electromagnetic Radiation," *Russian Journal of Applied Chemistry* 2015 (1976): 88–1980.

118. U. Basuli, S. Chattopadhyay, C. Nah, and T. K. Chaki, "Electrical Properties and Electromagnetic Interference Shielding Effectiveness of Multiwalled Carbon Nanotubes-Reinforced EMA Nanocomposites," *Polymer Composites* 33 (2012): 897–903.

119. S. S. Qavamnia and K. Nasouri, "Facile Fabrication of Carbon Nanotubes/Polystyrene Composite Nanofibers for High-Performance Electromagnetic Interference Shielding," *Fibers and Polymers* 2016 (1977): 17–1984.

120. K. Nasouri and A. M. Shoushtari, "Designing, Modeling and Manufacturing of Lightweight Carbon Nanotubes/Polymer Composite Nanofibers for Electromagnetic Interference Shielding Application," *Composites Science and Technology* 145 (2017): 46–54.

121. Y.-Q. Kang, M.-S. Cao, J. Yuan, and X.-Y. Fang, "Orientation-Dependent Electromagnetic Properties of Basalt Fibre/Nickel Core–Shell Heterostructures," *Chinese Physics B* 19, no. 1 (2010): 017701, https://doi.org/10.1088/1674-1056/19/1/017701.

122. Y.-Q. Kang, M.-S. Cao, J. Yuan, L. Zhang, B. Wen, and X.-Y. Fang, "Preparation and Microwave Absorption Properties of Basalt Fiber/Nickel Core–Shell Heterostructures," *Journal of Alloys and Compounds* 495 (2010): 254–259.

123. Y.-Q. Kang, M.-S. Cao, X.-L. Shi, and Z.-L. Hou, "The Enhanced Dielectric From Basalt Fibers/Nickel Core-Shell Structures Synthesized by Electroless Plating," *Surface and Coating Technology* 201 (2007): 7201–7206.

124. T. Si, S. Xie, Z. Ji, et al., "Modification of Basalt Fiber With Ni and Carbon Black Formed Synergistic Microstructure for Enhanced Electromagnetic Wave Absorption," *Journal of Materials Science: Materials in Electronics* 34 (2023): 1035.

125. I. V. Korotash, S. S. Polishchuk, and E. M. Rudenko, "Microwave Radiation Absorption in Heat-Resistant Basalt-Based Composites," *Applied Nanoscience* 13 (2023): 4989–4995.

126. S. Xu, Y. Shen, Q. Li, and X. Liu, "Hybrid Effects of Polyvinyl Alcohol (PVA) and Basalt Fibers on Microwave Absorption of Cement Composites With Fly Ash," *Journal of the American Ceramic Society* 104 (2021): 6345–6363.

127. T. Si, S. Xie, C. Ma, et al., "Microwave Absorption Properties of Double-Layer Structured Basalt Fiber/Resin Composites Containing Carbon Black and Nano-Fe_3O_4," *Composite Interfaces* 30 (2023): 959–981.

128. Y. Li, Y. Liu, Y. Cheng, and C. Jin, "Research on the Mechanical and Electromagnetic Properties of White Portland Cement Paste Containing Basalt Fiber," *Archives of Civil and Mechanical Engineering* 23 (2023): 63.

129. L. G. De Arco, Y. Zhang, A. Kumar, and C. Zhou, "Title of the Article," *IEEE Transactions on Nanotechnology* 8, no. 2 (2009): 135.

130. Z. Han, D. Li, X. Liu, D. Geng, J. Li, and Z. Zhang, "Microwave-Absorption Properties of Fe(Mn)/ferrite Nanocapsules," *Journal of Physics D: Applied Physics* 42 (2009): 055008.

131. G. Mittal and K. Y. Rhee, "Chemical Vapor Deposition-Based Grafting of CNTs Onto Basalt Fabric and Their Reinforcement in Epoxy-Based Composites," *Composites Science and Technology* 165 (2018): 84–94.

132. G. Mittal, K. Y. Rhee, and S. J. Park, "The Effects of Cryomilling CNTs on the Thermal and Electrical Properties of CNT/PMMA Composites," *Polymers (Basel)* 8 (2016): 169.

133. D. E. Dobry, D. M. Settell, J. M. Baumann, R. J. Ray, L. J. Graham, and R. A. Beyerinck, "A Model-Based Methodology for Spray-Drying Process Development," *Journal of Pharmaceutical Innovation* 4 (2009): 133–142.

134. M. Zhang, X. Qian, Q. Zeng, Y. Zhang, H. Cao, and R. Che, "Hollow Microspheres of Polypyrrole/Magnetite/Carbon Nanotubes by Spray-Dry as an Electromagnetic Synergistic Microwave Absorber," *Carbon N Y* 175 (2021): 499–508.

135. J. Liu, J. Xu, R. Che, H. Chen, M. Liu, and Z. Liu, "Hierarchical Fe_3O_4@TiO_2Yolk–Shell Microspheres With Enhanced Microwave-Absorption Properties," *Chemistry – A European Journal* 19 (2013): 6746–6752.

136. M. Kim, T.-W. Lee, S.-M. Park, and Y. G. Jeong, "Structures, Electrical and Mechanical Properties of Epoxy Composites Reinforced With MWCNT-Coated Basalt Fibers," *Composites. Part A, Applied Science and Manufacturing* 123 (2019): 123–131.

137. J. Orava, T. Kohoutek, and T. Wagner, "Deposition Techniques for Chalcogenide Thin Films," in *Chalcogenide Glasses*, eds. J.-L. Adam and X. Zhang (Cambridge: Woodhead Publishing, 2014), 265–309.

138. T. Scalici, G. Pitarresi, D. Badagliacco, V. Fiore, and A. Valenza, "Mechanical Properties of Basalt Fiber Reinforced Composites Manufactured With Different Vacuum Assisted Impregnation Techniques," *Composites Part B: Engineering* 104 (2016): 35–43.

139. M. Barczewski, J. Aniśko, A. Piasecki, et al., "The Accelerated Aging Impact on Polyurea Spray-Coated Composites Filled With Basalt Fibers, Basalt Powder, and Halloysite Nanoclay," *Composites Part B: Engineering* 225 (2021): 109286.

140. M. Shateri-Khalilabad and M. E. Yazdanshenas, "Fabricating Electroconductive Cotton Textiles Using Graphene," *Carbohydrate Polymers* 96 (2013): 190–195.

141. M. R. Nateghi and M. Shateri-Khalilabad, "Silver Nanowire-Functionalized Cotton Fabric," *Carbohydrate Polymers* 117 (2015): 160–168.

142. T.-W. Lee, S.-E. Lee, and Y. G. Jeong, "Highly Effective Electromagnetic Interference Shielding Materials Based on Silver Nanowire/Cellulose Papers," *ACS Applied Materials and Interfaces* 8 (2016): 13123–13132.

143. T.-W. Lee, S.-E. Lee, and Y. G. Jeong, "Carbon Nanotube/Cellulose Papers With High Performance in Electric Heating and Electromagnetic Interference Shielding," *Composites Science and Technology* 131 (2016): 77–87.

144. J. Yu, Z. Cui, J. Lu, et al., "Integrated Hierarchical Macrostructures of Flexible Basalt Fiber Composites With Tunable Electromagnetic Interference (EMI) Shielding and Rapid Electrothermal Response," *Composites Part B: Engineering* 224 (2021): 109193.

145. X. Li, X. Yin, C. Song, et al., "Self-Assembly Core–Shell Graphene-Bridged Hollow MXenes Spheres 3D Foam With Ultrahigh Specific EM Absorption Performance," *Advanced Functional Materials* 28 (2018): 1803938.

146. H. Duan, P. He, H. Zhu, Y. Yang, G. Zhao, and Y. Liu, "Constructing 3D Carbon-Metal Hybrid Conductive Network in Polymer for Ultra-Efficient Electromagnetic Interference Shielding," *Composites Part B: Engineering* 212 (2021): 108690.

147. B. Lu, H. Huang, X. L. Dong, et al., "Influence of Alloy Components on Electromagnetic Characteristics of Core/Shell-Type Fe–Ni Nanoparticles," *Journal of Applied Physics* 104 (2008): 114313.

148. H. Guo, Y. Zhan, Z. Chen, F. Meng, J. Wei, and X. Liu, "Decoration of Basalt Fibers With Hybrid Fe_3O_4 microspheres and Their Microwave Absorption Application in Bisphthalonitrile Composites," *Journal of Materials Chemistry A* 1 (2013): 2286–2296.

149. Y. Liu, Y. Yang, Z. Yang, Y. Liu, Y. Su, and J. Niu, "Influence of the Thickness of Graphene Coating on the Electromagnetical and Mechanical Properties of Double-Layer Coated Basalt Fibre Fabrics," *Fibres and Textiles in Eastern Europe* 28, no. 5 (2020): 69–74.

150. V. Dhand, C. Hyunsuk, T. Hassan, C. M. Koo, and K. Y. Rhee, "Tailored Eutectic Alloy Coating for Enhanced EMI and X-Ray Protection by Basalt Fiber CNT/Epoxy Composite," *Journal of Materials Research and Technology* 31 (2024): 689–697.

151. R. Alwafi and A. Saeed, "Single-Walled Carbon Nanotubes in Nanosized Basalts as Nanocomposites: The Electrical/Dielectric Properties and Electromagnetic Interference Shielding Performance," *Journal of Inorganic and Organometallic Polymers and Materials* 32 (2022): 4340–4358.

152. S. Ghosh, S. Ganguly, S. Remanan, and N. C. Das, "Fabrication and Investigation of 3D Tuned PEG/PEDOT: PSS Treated Conductive and Durable Cotton Fabric for Superior Electrical Conductivity and Flexible Electromagnetic Interference Shielding," *Composites Science and Technology* 181 (2019): 107682.

153. K. Rajavel, X. Yu, P. Zhu, Y. Hu, R. Sun, and C. Wong, "Exfoliation and Defect Control of Two-Dimensional Few-Layer MXene $Ti_3C_2T_x$ for Electromagnetic Interference Shielding Coatings," *ACS Applied Materials and Interfaces* 12 (2020): 49737–49747.

154. F. Bian, R. Huang, X. Li, J. Hu, and S. Lin, "Facile Construction of Chestnut-Like Structural Fireproof PDMS/Mxene@BN for Advanced Thermal Management and Electromagnetic Shielding Applications," *Advanced Science* 11 (2024): 2307482.

155. K. Markandan and C. Q. Lai, "Fabrication, Properties and Applications of Polymer Composites Additively Manufactured With Filler Alignment Control: A Review," *Composites Part B: Engineering* 256 (2023): 110661.

156. A. J. Robinson, A. Pérez-Nava, S. C. Ali, J. B. González-Campos, J. L. Holloway, and E. M. Cosgriff-Hernandez, "Comparative Analysis of Fiber Alignment Methods in Electrospinning," *Matter* 4 (2021): 821–844.

157. E. Rezvani Ghomi, F. Khosravi, R. E. Neisiany, et al., "Advances in Electrospinning of Aligned Nanofiber Scaffolds Used for Wound Dressings," *Biomedical Engineering* 22 (2022): 100393.

158. L. Tian, H. Gu, Q. Zhang, et al., "Multifunctional Hierarchical Metamaterial for Thermal Insulation and Electromagnetic Interference Shielding at Elevated Temperatures," *ACS Nano* 17 (2023): 12673–12683.

159. M. L. Hakim, T. Alam, and M. T. Islam, "Polarization-Insensitive and Oblique Incident Angle Stable Miniaturized Conformal FSS for 28/38 GHz Mm-Wave Band 5G EMI Shielding Applications," *IEEE Antennas and Wireless Propagation Letters* 22 (2023): 2644–2648.

160. S. M. Zachariah, T. Antony, Y. Grohens, and S. Thomas, "From Waste to Wealth: A Critical Review on Advanced Materials for EMI Shielding," *Journal of Applied Polymer Science* 139 (2022): e52974.

161. Z. Cheng, R. Wang, Y. Wang, et al., "Recent Advances in Graphene Aerogels as Absorption-Dominated Electromagnetic Interference Shielding Materials," *Carbon N Y* 205 (2023): 112–137.

162. K. Sushmita, D. Ghosh, S. Nilawar, and S. Bose, "Absorption Dominated Directional Electromagnetic Interference Shielding Through Asymmetry in a Multilayered Construct With an Exceptionally High Green Index," *ACS Applied Materials and Interfaces* 14 (2022): 49140–49157.